GCAGS JOURNAL
A Publication of the Gulf Coast Association of Geological Societies
www.gcags.org

Depositional Systems, Lithofacies, and Lithofacies Stacking Patterns of the Jurassic Smackover Formation (Oxfordian) and Buckner Anhydrite (Kimmeridgian) in Van Zandt County, Texas: A Type-Cored Section from Northeastern Texas

Peter Schemper[1], Robert G. Loucks[2], and Qilong Fu[2]

[1]*ExxonMobil, ExxonMobil Houston Campus, Springwoods Village Pkwy., Spring, Texas 22777, U.S.A.*

[2]*Bureau of Economic Geology, Jackson School of Geosciences, University of Texas at Austin, Box X, University Station, Austin, Texas 78713–8924, U.S.A.*

ABSTRACT

The Jurassic Smackover Formation and Buckner Anhydrite compose a widespread petroleum system along the onshore northern Gulf of Mexico. This system comprises a thick sequence of carbonate and evaporite strata deposited on a gently sloping ramp in a semi-enclosed basin between North and South America. The general climate was arid, which is reflected in the lithofacies deposited. The Smackover section is generally divided into three intervals that reflect inner, middle, and outer ramps. The lower Smackover section was deposited in a deeper water (below storm-wave base) outer-ramp setting. Sedimentation was dominated by low-energy, dysoxic to anoxic mud-dominated lithofacies punctuated by gravity-flow deposits. The outer ramp is the major source rock for the Smackover reservoirs, and much of the organic matter is associated with anoxically deposited microbial mats. Middle Smackover sediments on the middle ramp were deposited under oxic conditions varying from below- to above-storm-wave base. Living conditions of biota improved relative to the outer-ramp setting, as evidenced by extensive bioturbation. Upper Smackover sedimentation in the inner ramp produced a mosaic of lithofacies deposition under oxic, low- to high-energy conditions. The Buckner Anhydrite is separated from the Smackover Formation by an unconformity and is dominated by evaporite deposition in various settings ranging from salina to sabkha, with influences from eolian and wadi depositional processes. The investigated core, Sun No. 1 Travis Gas Unit in Van Zandt County, is proposed as the type-cored section of the Smackover Formation–Buckner Anhydrite in northeastern Texas. The range in lithofacies in the core covers the spectrum of types seen in the Smackover Formation–Buckner Anhydrite trend along the onshore northern rim of the Gulf of Mexico.

INTRODUCTION

The Upper Jurassic Smackover Formation (Fig. 1) is part of a prolific petroleum system along the onshore northern rim of the Gulf of Mexico (Fig. 2) that has a long history of exploration and production (e.g., Budd and Loucks, 1981; Moore, 1984; Oehler, 1984; Ewing, 2001; Mancini et al., 2003; Pearson, 2011). Most investigations of the Smackover Formation have examined on-shelf subbasins east of the East Texas Basin, primarily focusing on upper Smackover oolitic grainstone reservoirs. Only a few studies have investigated the complete Smackover ramp section, especially the lower Smackover source-rock section. Because of this, little is known about the conditions under which much of the middle and lower Smackover strata were deposited. In addition, with unconventional plays now being active reservoir targets, the lower Smackover section has become of prime interest (e.g., Brown Dense Dolomite (Barnaby, 2013; Yang et al., 2015)). In the present investigation, a continuous long (713 ft [217.3 m]) core from Van Zandt County, Texas (Figs. 2 and 3)—the Sun Oil No. 1 Travis Gas Unit—is available for characterizing a nearly complete section of the Smackover and much of the Buckner Anhydrite section. This well had an initial production of 13,639 million cubic ft per day (MMcf/d) of natural gas in the upper Smackover section from 13,357 to 13,485 ft (4071.2 to 4110.2 m) (IHS Markit Inc., 2022).

Manuscript received April 25, 2022; revised manuscript received July 26, 2022; manuscript accepted July 26, 2022.

GCAGS Journal, v. 11 (2022), p. 16–36.

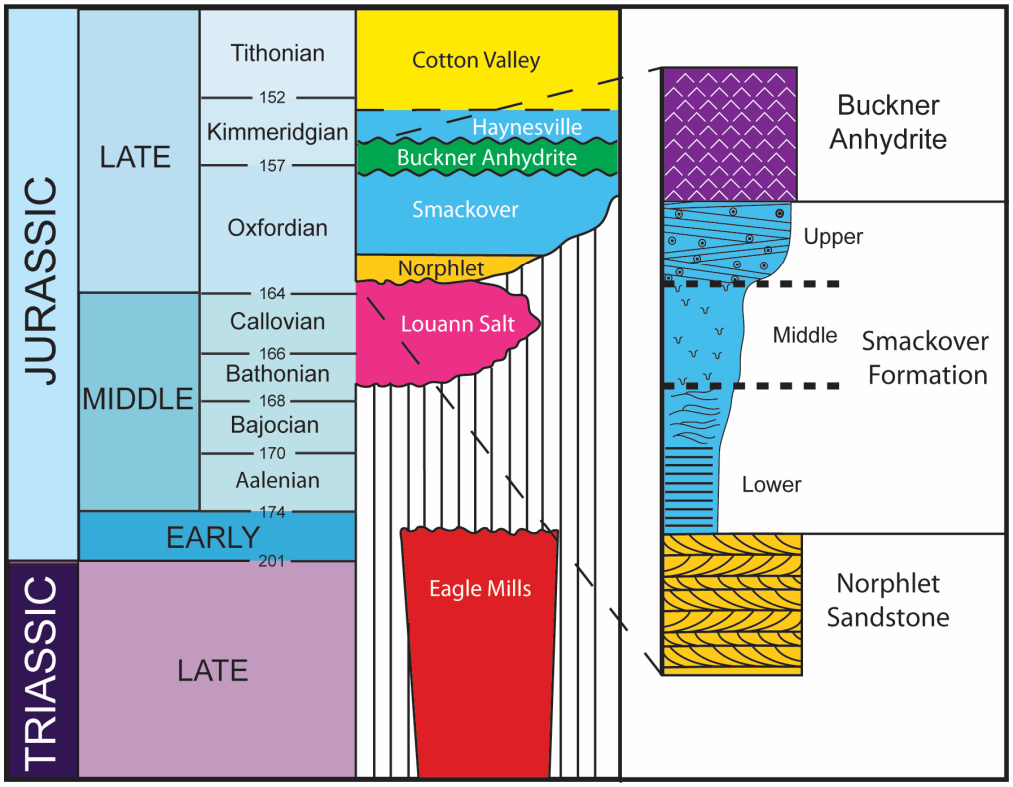

Figure 1. Stratigraphic section of the Late Triassic and Jurassic, northeastern Texas (modified after Heydari and Baria [2005]). Dates, in millions of years, are from Walker et al. (2018).

The primary goal of this investigation is to characterize the Smackover Formation and Buckner Anhydrite to create a type-cored section for use by future studies, and to create a refined depositional model for East Texas Smackover and Buckner Anhydrite. Specific objectives are to: (1) review the regional depositional setting of northeastern Texas during Late Jurassic time, (2) define the spectrum of lithofacies that compose the Smackover Formation and Buckner Anhydrite sections as well as the depositional environments in which they formed, (3) develop a depositional model for the Smackover section for northeastern Texas area, (4) and comment on the Sun Oil No. 1 Travis Gas Unit core as a type-cored section for northeastern Texas.

This investigation of the Smackover–Buckner petroleum system will provide additional geological insights and concepts for the continued exploration along the Gulf of Mexico as well as underexplored areas such as South Texas and the Mexican eastern continental margin. This type core can be used to compare and contrast lithofacies and lithofacies stacking patterns throughout the Gulf of Mexico region.

DATA AND METHODS

The major source of data used in this investigation is a continuous long (713 ft [217.3 m]) core from Van Zandt County, Texas (Figs. 2–5) and associated wireline logs. The core is from the Sun No. 1 Travis Gas Unit (current operator Oryx Energy Co.; API# 42467012620000) that was drilled in 1968. The core contains 87% (592 ft [180.4 m]) of the Smackover Formation (lower 85 ft [26 m] not cored) and 80% of the overlying Buckner Anhydrite (121 ft [36.9 m]). A nearly complete spectrum of Smackover and Buckner Anhydrite lithofacies was cored.

Before we conducted a detailed core description, the core was slabbed and lightly etched with hydrochloric acid. The acid cleans off saw marks and emphasizes features in slight-relief insoluble minerals. The slabbed core was described using a binocular microscope to record lithofacies and their characteristics. Dunham's (1962) carbonate classification was used to classify the texture and fabric of the lithofacies.

Eighty-seven thin sections were prepared to supplement the core description. Thin sections were impregnated with blue epoxy to emphasize megapores under plain light and blue-fluorescence dye to identify micropores under ultraviolet light. A petrographic microscope was used to define depositional texture, fabric, mineralogy, sedimentary structures, and grain types.

Twenty-eight rock samples were analyzed for organic-matter characterization by GeoMark Research, Ltd., in Houston, Texas. Samples were analyzed for total organic carbon (TOC) and kerogen properties using Leco TOC and Rock-Eval pyrolysis. TOC analysis was run on a LECO C230 instrument and Rock-Eval on a Rock-Eval II instrument, respectively.

Energy-dispersive X–ray fluorescence (XRF) data were collected at 2 in (5 cm) intervals along the full length of the core for 10 major elements and 20 trace elements. The XRF analysis was completed using a Bruker AXS Tracer III–V XRF handheld unit. This unit was calibrated for both major and trace-element analysis using methodology outlined by Rowe et al. (2012). The core was scanned for major elements using 15 kV for 60 sec and for trace elements using 40 kV for 90 sec. In this investigation, only Ca and Mg analyses are used.

STRATIGRAPHY AND GENERAL REGIONAL GEOLOGY

Stratigraphy

Figure 1 shows the stratigraphy in the area of investigation. The Smackover Formation (Oxfordian) unconformably overlies the siliciclastic Norphlet Formation (Oxfordian) and unconformably underlies the Buckner Anhydrite (Kimmeridgian) in the core used in this study. The time period represented by the core is ~8 million yr (Fig. 1). Internally, the Smackover Formation is divided into the lower, middle, and upper units (e.g., Dickinson, 1968,

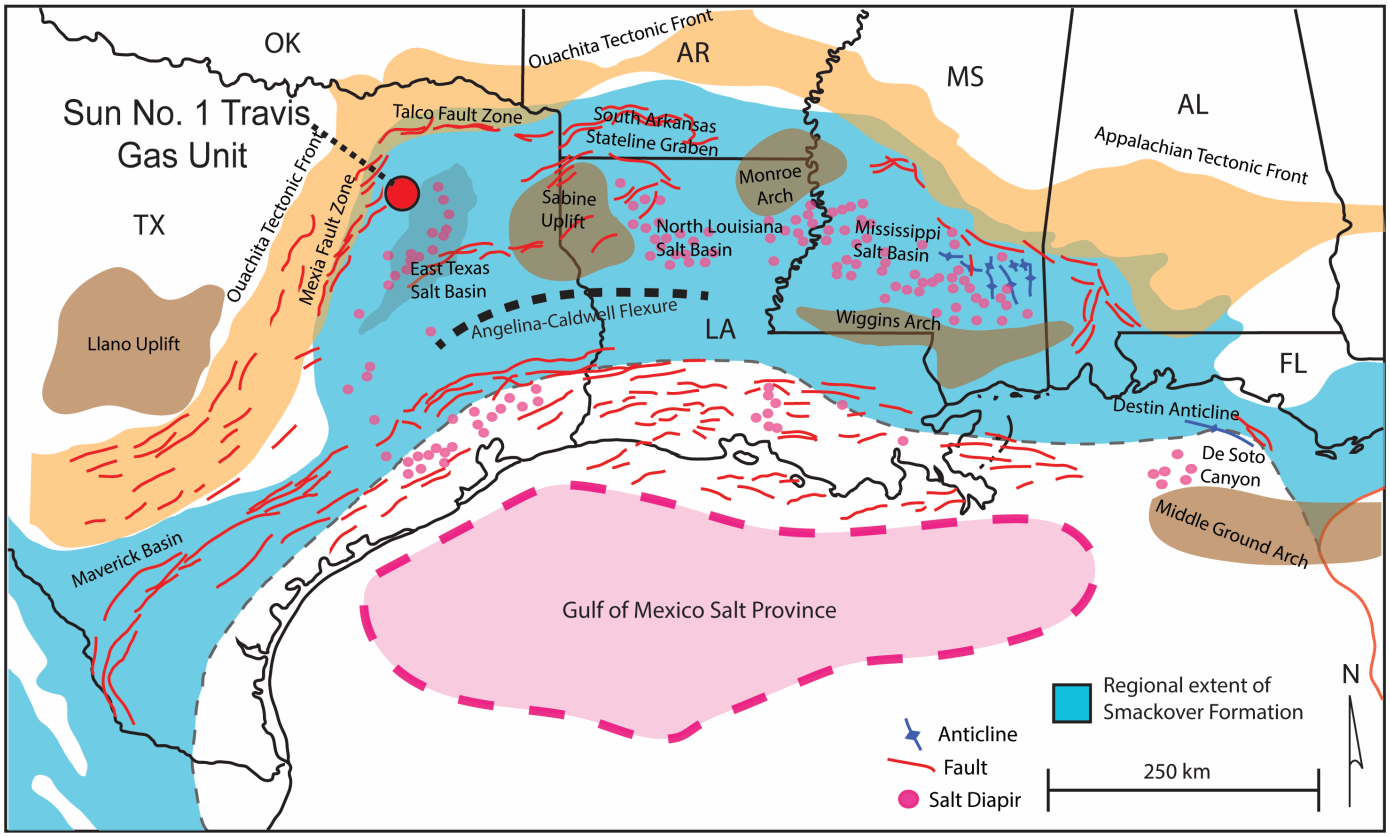

Figure 2. Map of major structural features along the northern Gulf of Mexico (modified after Martin [1978]). Regional extent of the Smackover Formation is shown. Red circle shows the location of the Sun No. 1 Travis Gas Unit.

1969). This investigation will show that the Smackover deposition was not continuous but instead contained several unconformities related to eustatic sea-level changes, which would be expected in an 8 million yr time period.

General Regional Geology

Dominant structural features controlling the deposition of Upper Jurassic sediments in northeastern Texas formed during rifting events in the Late Triassic to Middle Jurassic, which resulted in the formation of the Gulf of Mexico (Pilger, 1981; Jackson, 1982; Ewing, 2001; Pindell and Kennen, 2001) (Fig. 2). A series of failed rift zones landward of the main rifting event led to the formation of salt basins along the modern-day northern onshore Gulf of Mexico (Jackson and Seni, 1983) (Fig. 2). The basins are separated by elevated basement features that are interpreted as areas of little to no rifting or extension of the lithosphere (Ewing, 2009) (Fig. 2). Linear elevated features such as the Angelina Caldwell Flexure (Toledo Bend Flexure) and the Wiggins Arch separated the interior basins from the Gulf of Mexico and may have restricted the basins from receiving a steady influx of seawater (Wood and Walper, 1974) (Fig. 2).

The East Texas Basin is bounded on its east by the Sabine Uplift and to its west and north by the Mexia and Talco fault zones (Jackson, 1982) (Fig. 3). These fault zones are aligned with the updip edge of the Louann Salt (Jackson, 1982). Migration of basinal salts is interpreted as starting toward the end of Smackover deposition as Jurassic sediments began to prograde into the basin. Mobilization of the salt created complex structural features and faulting that impacted sedimentation throughout the East Texas Basin (Jackson, 1982). Faulting in the Mexia-Talco Fault Zone and basinal salt structures developed from the Late Jurassic to Early Cretaceous (Jackson and Seni, 1983).

The earliest sediments within the East Texas Basin were Triassic and Lower Jurassic red beds of the Eagle Mills Formation (Heydari and Baria, 2005) (Fig. 1). In the late middle Jurassic (Bathonian-Callovian), a transgression led to the formation of restricted hypersaline conditions, depositing the massive Louann Salt and its updip equivalent, the Werner Formation (Salvador, 1987; Harwood and Fontana, 1983). After deposition of the Louann and Werner Formations, a regional sea-level lowstand led to the deposition of the Norphlet siliciclastics (Wade and Moore, 1993) (Fig. 1).

After Norphlet deposition, a second-order transgressive event led to the deposition of the Smackover Formation (Goldhammer, 1998) (Figs. 1 and 6A). As shown in Figure 6A, the Smackover trend in northeastern Texas forms a facies belt that is bordered updip by alluvial siliciclastic strata and downdip by the deeper water Louark basinal limestones and black shales.

In most parts of the East Texas Basin the Smackover section is overlain by the Buckner Anhydrite, the updip part of the Haynesville Group (Stewart, 1984) (Figs. 1 and 6B). The Haynesville Group is composed of the Buckner Anhydrite, upper Buckner, Gilmer limestones, and Gilmer shale (Stewart, 1984). As shown in Figure 6B, the Buckner Anhydrite is not continuous; it is centered in northeasternmost Texas. The Haynesville siliciclastics form a continuous trend landward of the Buckner Anhydrite, and the Gilmer and Cotton Valley carbonate strata form a broad shelf seaward. The Louark basinal limestones and black shales stepped seaward relative to their position during Oxfordian time.

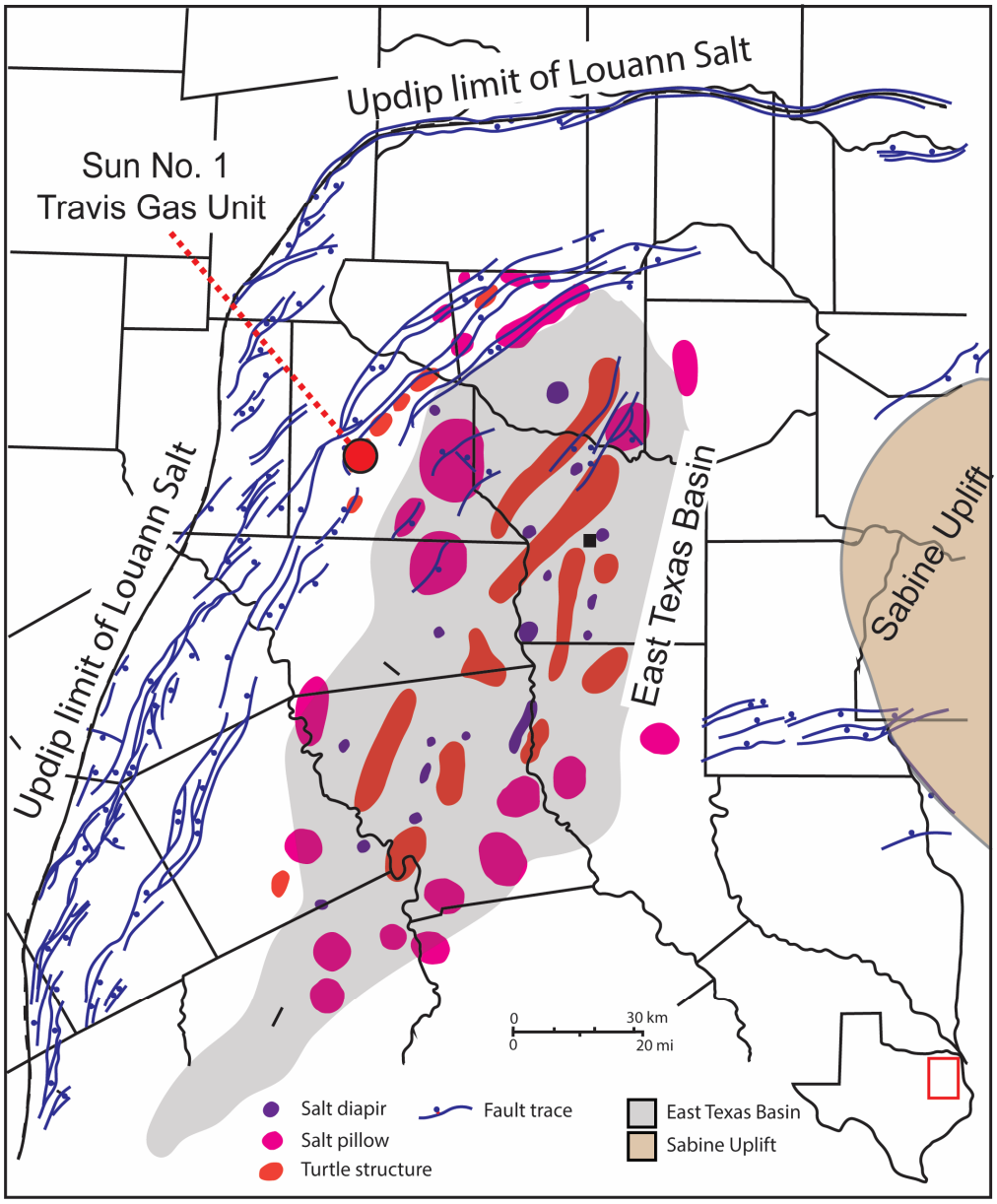

Figure 3. Structural features of the East Texas Basin (modified after Jackson [1982]).

Within the literature a debate exists regarding the contact between the Smackover Formation and the overlying Buckner Anhydrite (Fig. 1). Some authors interpreted it as conformable (Mitchell-Tapping, 1984; Hancharik, 1984; Mann, 1988), and others suggested that it is unconformable (Moore, 1997; Heydari and Baria, 2005). In the studied core, the contact is unconformable, as the uppermost Smackover section has been eroded and capped by caliche formation. The unconformity is interpreted to be related to erosion during salt movement.

SMACKOVER AND BUCKNER ANHYDRITE LITHOFACIES

Approach to Describing Lithofacies

A complete core description of the Smackover and Buckner sections in the Sun No. 1 Travis Gas Unit core is presented in Figures 4 and 5. Ten lithofacies were differentiated in the Smackover section, and six lithofacies were differentiated in the Buckner Anhydrite section. In some intervals, dolomitization and anhydrite replacement obscured rock fabric. Alongside the Smackover core description is a plot showing the XRF values of elemental abundances of Ca (blue) and Mg (purple). In general, high values of Ca are a proxy for calcite, and high values of Mg are a proxy for dolomite. TOC abundance, which is a strong proxy for defining whether the sea bottom was oxic, dysoxic, or anoxic (Arthur and Sageman, 1994), is also described here, because TOC content is important in describing lithofacies and interpreting their depositional environment. These data are contextualized by Rock-Eval pyrolysis organic matter analyses, which additionally provide insight into source-rock potential (Fig. 7).

The general depositional setting of the Smackover and Buckner Anhydrite section was a ramp (Fig. 8) dipping into the Gulf of Mexico (e.g., Ahr, 1973; Budd and Loucks, 1981; Ewing, 2001; Heydari and Baria, 2005). Therefore, the lithofacies are presented in context of this well-established depositional model of the Smackover–Buckner Anhydrite section.

Lithofacies are ordered from the oldest section (lower Smackover Formation) to the youngest section (Buckner Anhy-

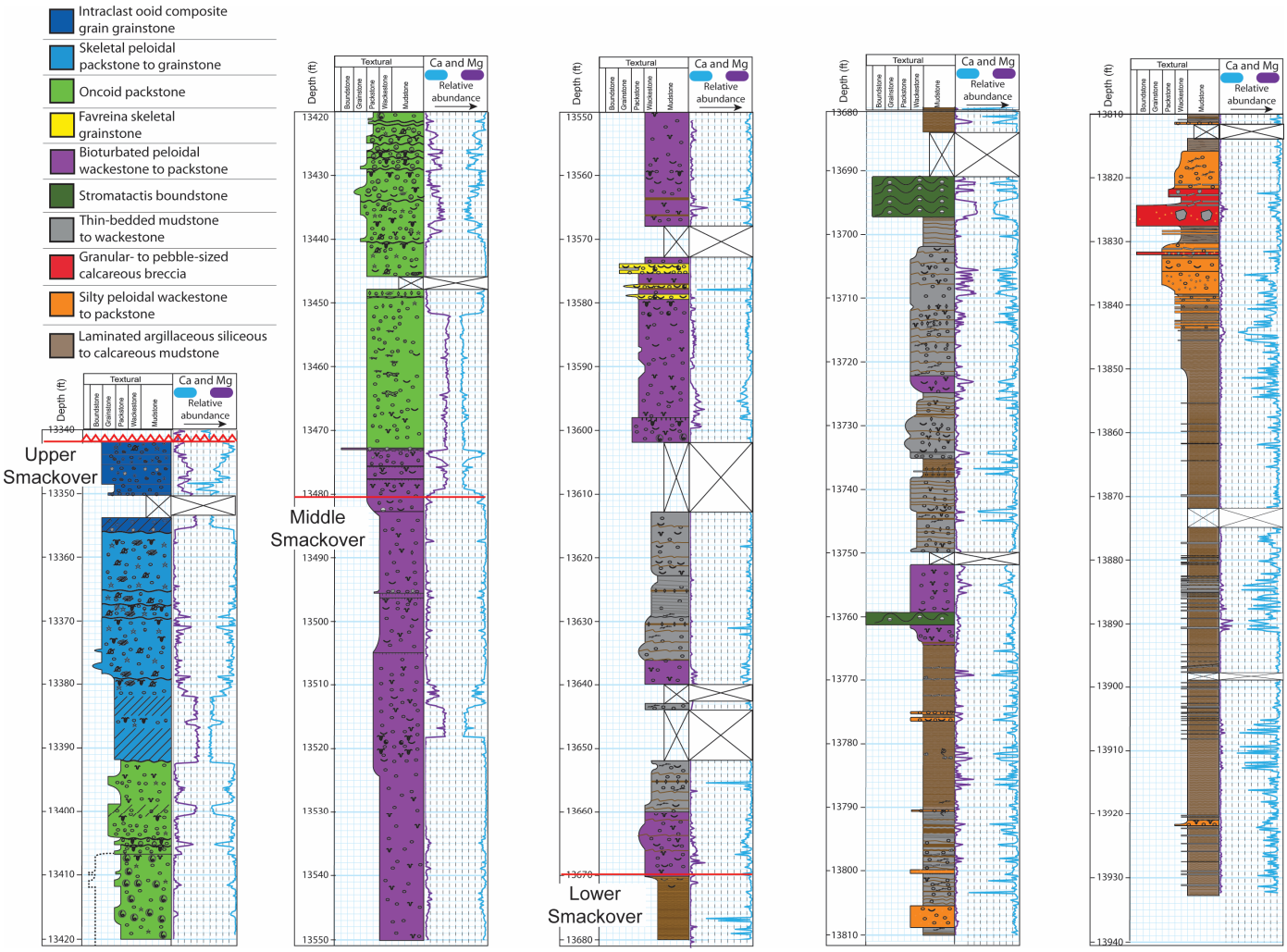

Figure 4. Core description of the Smackover section, Sun No. 1 Travis Gas Unit. Tops of inner, middle, and outer Smackover units are marked. See Figure 5 for legend.

drite). Our approach is first to describe the lithofacies as to their defining characteristics and then interpret the depositional environment. We think this is the most efficient and comprehensive approach to understanding the lithofacies, while keeping description (i.e., data) separated from interpretations. Because we would like this core to be considered as the type-cored section for the Smackover and Buckner formations in this area, we describe the lithofacies in detail.

Total Organic Carbon

Sample locations used in organic-matter analysis were selected targeting intervals with dark color, low carbonate content, and few dissolution seams in order to emphasize organic-rich zones. Rock-Eval analysis was performed concurrently with TOC measurements to evaluate source-rock properties and potential; however, the analyses showed that the Smackover samples have very low hydrogen index (HI) values (mean = 7.4 mg HC/g TOC) (Fig. 7B), reflecting the elevated thermal maturities that the organics underwent during burial. As a result of the low HI values, vitrinite reflectance (R_o) and temperature of maximum rate of hydrocarbon production from kerogen cracking during pyrolysis (T_{max}) values could not be calculated (except for one sample), and kerogen type could not be well identified using a pseudo–van Krevelen plot (Fig. 7B). The one T_{max} value of 460° C (860°F) was analyzed, and this is equivalent to a calculated R_o of 1.1%, which is well into the dry gas window; however, R_o could have been much higher. Caution should be used with this Rock-Eval data for R_o because it is questionable. Although our samples could not accurately identify kerogen type, it is worth noting that a regional study by Sassen (1990) identified oil generated by type 1 kerogen from lower Smackover source strata near the study area. This kerogen type correlates well with anoxically deposited microbial mats in the lower Smackover interval, as described below.

The average TOC value is 0.48 wt% and the highest value is 1.59 wt% in the investigated samples (Fig. 7A). Higher TOC values correspond to samples with low percent carbonate. A $S_1 + S_2$ vs. TOC plot was generated (Fig. 7A) to evaluate source-rock quality. The $S_1 + S_2$ values, all less than 1 mg HC/g rock, indicate that the lower Smackover strata in this well appear to have poor source-rock quality. However, as noted above, this may be the result of high thermal maturity, and these strata may have originally had good source-rock quality, as noted by Sassen (1990). The TOC values in the plot show that nearly half the samples have fair to good amounts of TOC (Fig. 7A). Preservation of fair to moderate amounts of TOC in the lower Smackover indicates that dysoxic to anoxic conditions existed, and this com-

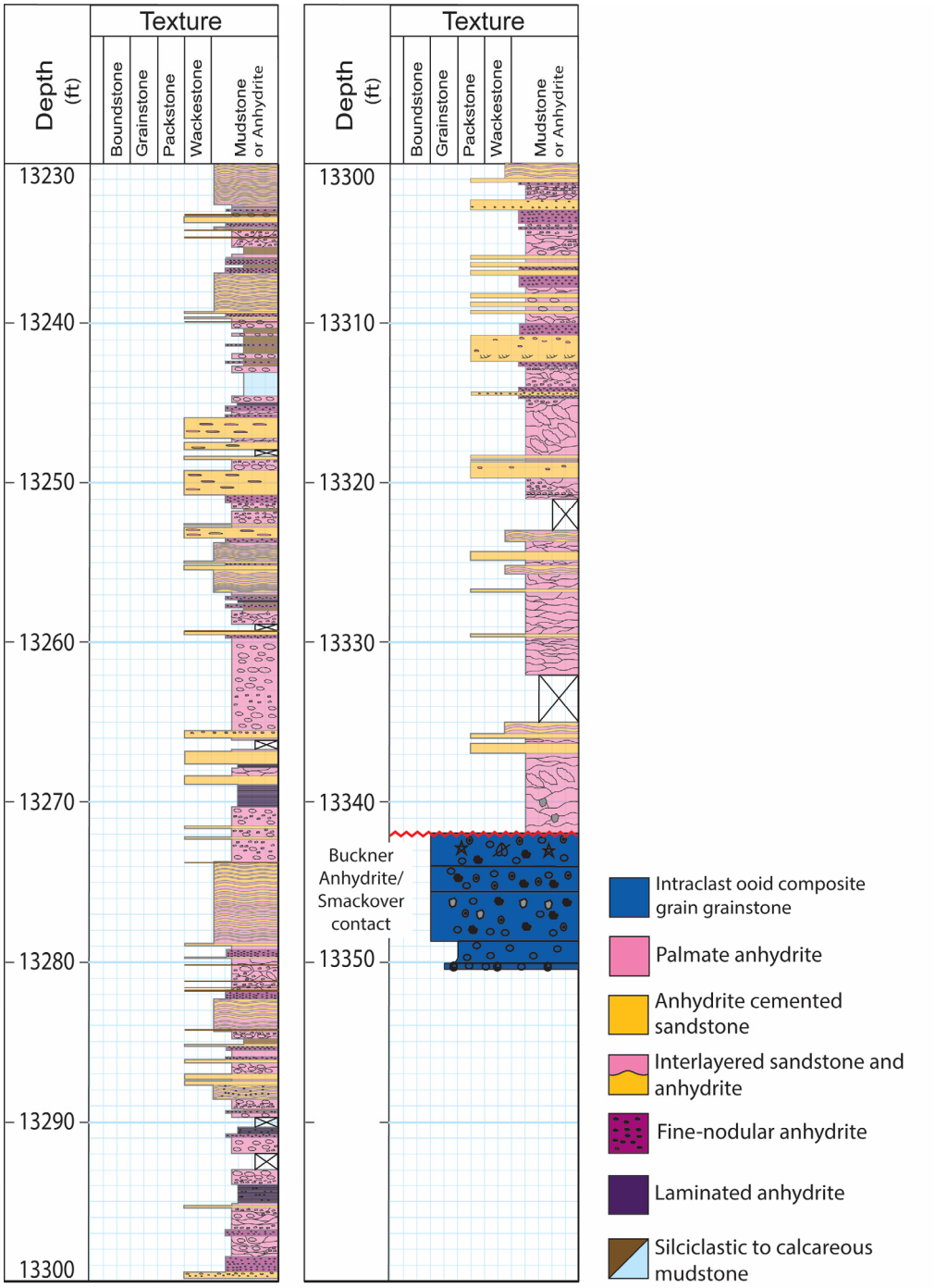

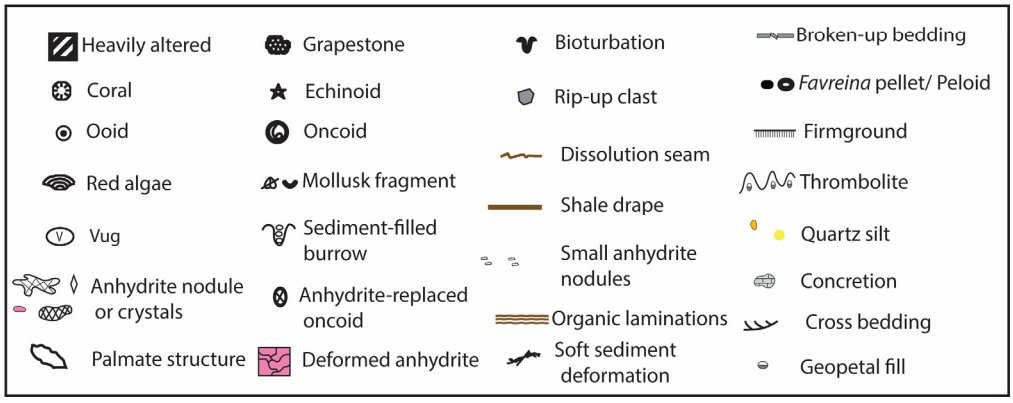

Figure 5. Core description of the Buckner Anhydrite section, Sun No. 1 Travis Gas Unit. Contact between the Smackover Formation and Buckner Anhydrite is shown.

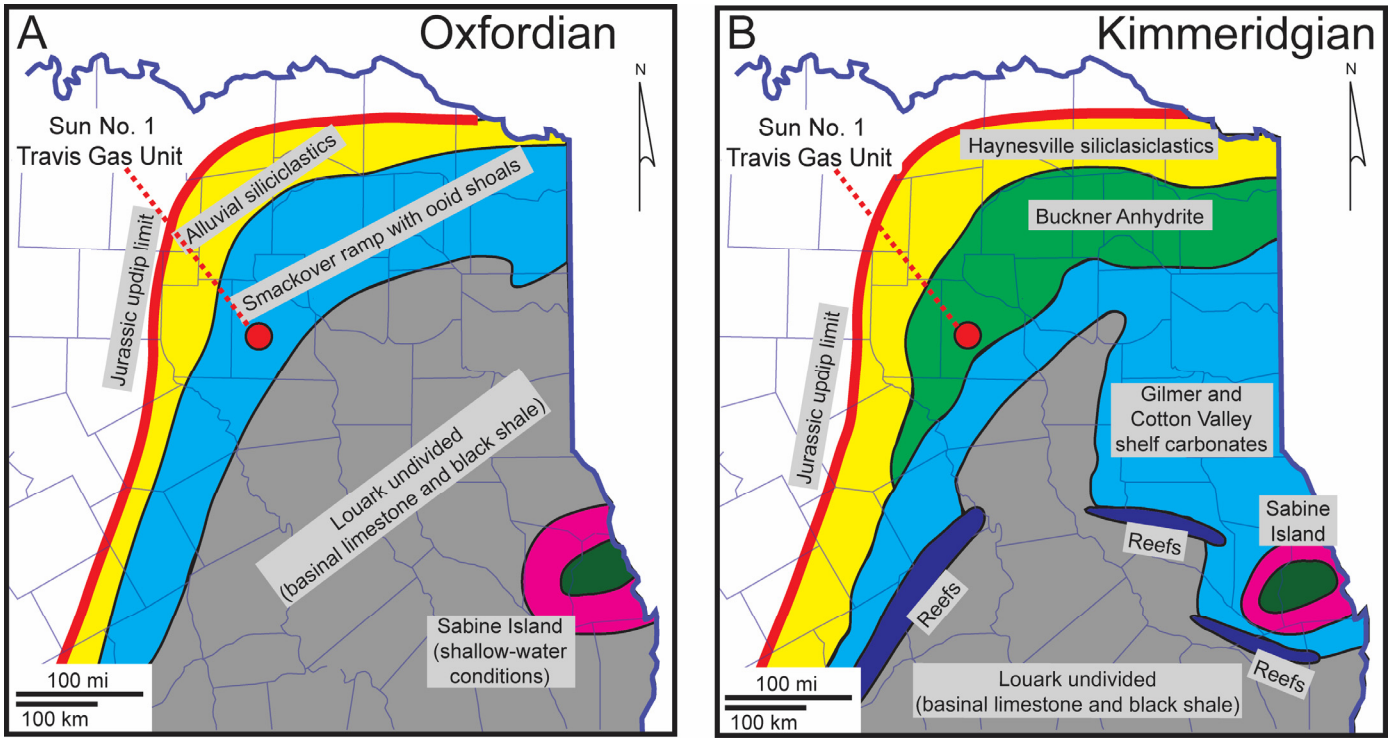

Figure 6. General regional lithofacies maps, Oxfordian (A) and Kimmeridgian (B) time periods. Red circle shows the location of the Sun No. 1 Travis Gas Unit. Maps modified and generalized from Ewing (2001).

pares well with lack of benthic biota and bioturbation, well-developed microbial mats, well-laminated strata, and abundant pyrite.

A box plot (Fig. 7C) compares the amount of TOC between the major Smackover units and Buckner Anhydrite. Within the Smackover Formation, the lower Smackover has the highest amount of TOC, and the upper Smackover has the lowest amount. This upward decrease in abundance of TOC through the Smackover section correlates with the change from anoxic conditions in the lower Smackover into oxic conditions in the upper Smackover.

Oxygenation distribution of the Smackover section is discussed below. The Buckner Anhydrite also has a low amount of TOC but more than in the upper Smackover section, indicating that the evaporitic environment was stressed and had limited biota to consume the kerogen.

Lower Smackover Formation Lithofacies

Laminated Argillaceous to Calcareous Mudstone (Laminated Mudstone)

Description: The lithofacies is composed of three distinct bedding styles: millimeter-scale laminae of quartz-silt and organic-rich layers (Figs. 9A, 9D, 9F, and 9G), millimeter- to centimeter-scale carbonate-rich laminae with some microbial mats (Fig. 9E), and thin-bedded carbonate mudstones (Fig. 9C). The quartz-silt and organic-rich laminae alternate with the carbonate-rich laminae at the scale of several millimeters to thin packages that are centimeters thick. Some laminae pinch out and laterally transition between the different types (Figs. 9A, 9D, and 9G). Vertical contacts between laminae are sharp.

The carbonate-rich laminae are generally capped by parallel and continuous layers of quartz silt (Fig. 9D) and in some cases, higher up in the cored section, *Favreina* pellets (i.e., shrimp pellets) are present. The laminated beds show several features, including planar lamination, wavy lamination, discontinuous disrupted lamination, low-angle ripple cross-laminae, and small-scale compressional structures such as small folds and millimeter-scale microfaults (Fig. 9F). Within the laminated organic matter, microfolding is observed (as overturned microbial mats) (Fig. 9G). The laminated intervals contain an abundance of pyrite microframboids, ranging from 2 to 20 microns in size, that are observed replacing organics-rich sediment.

The thin-bedded carbonate mudstones range in thickness from 1.2 to 6.3 in (3 to 16 cm) and form abrupt contacts with the laminated layers (Fig. 9B). These beds commonly contain upward-fining sequences and current and traction hydrodynamic features such as peloidal lags, ripples, and scour surfaces as well as current-related laminae.

Abundant fractures ranging from 0.04 to 1 in (1 mm to 2.5 cm) wide and 1.2 to 5.9 in (3 to 15 cm) long are confined to the more carbonate-rich intervals (Fig. 9A). Some fractures are filled by coarse-crystalline calcite, dolomite, and sulfide-rich cements (Fig. 10A). Most of the fractures are wavy ptygmatic fractures, indicating formation during early compaction (Fig. 9A). Additionally, injection features of carbonate-poor muds filling early formed fractures in carbonate beds are common.

Interpretation: Preservation of laminae and microbial mats, little to no bioturbation, pyrite microframboids, and lack of benthic organisms indicate that the environment of deposition was in a distal, lower energy anoxic bottom setting. Additionally, there is a lack of skeletal grains and peloids from organisms living within the water column, aside from minor amounts of *Favreina* pellets that were likely transported from shallower settings by gravity-flow currents. This suggests that the water column may have also been stressed and was probably related to elevated salinities. Organic matter that is interlaminated with the carbonate muds and quartz silts is interpreted as being formed by sulfur reducing microbial mats. This interpretation is based on observations of continuous and parallel organic laminae, over-

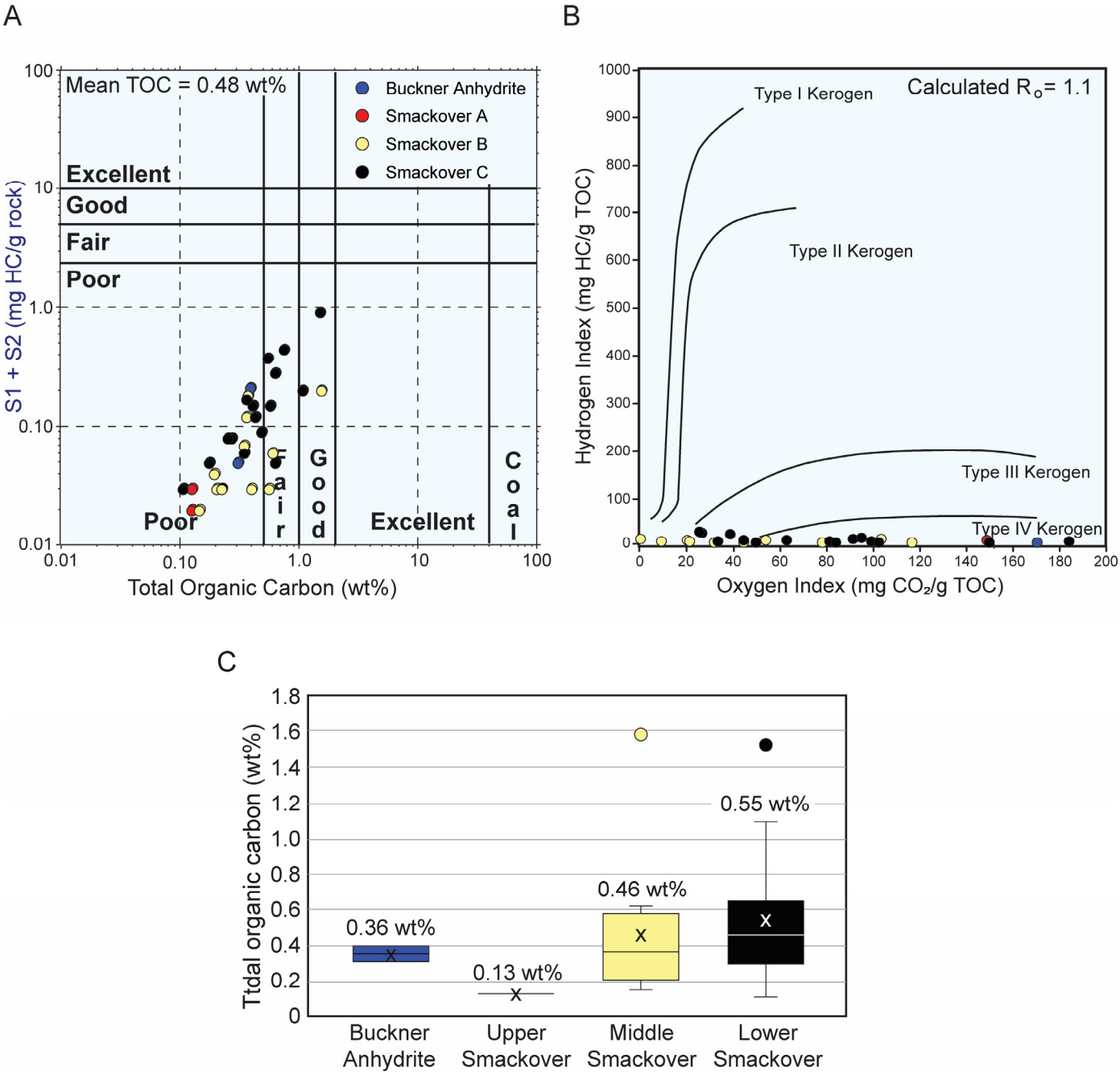

Figure 7. Source-rock-quality analysis. (A) S1 + S2 versus total organic carbon (TOC) plot. Data show relatively poor S1 + S2 values but many fair to good TOC values. R_o of 1.1 (possibly higher) suggests that the kerogen has been degraded by high thermal maturity. Values are separated by stratigraphic units. (B) Pseudo–van Krevelen kerogen-type diagram. All data show very low HI index resulting from thermal degradation. (C) Box plot comparing TOC by units. Box = interquartile range, horizontal line in box = median, X = mean, and vertical line = minimum to maximum range.

turned mats (Fig. 9G), and rip-up mat clasts (Fig. 10E), and also on biomarker studies discussed in the literature (Claypool and Mancini, 1989; Sassen, 1990) in other lower Smackover sections. This interpretation is similar to those made by Budd and Loucks (1981) in South Texas, Heydari et al. (1997) in Arkansas and Mississippi, Moore (1997) in southern Arkansas, and Harwood and Fontana (1983) in East Texas. The quartz grains in the parallel and continuous laminae are interpreted to have been transported by eolian (i.e., windblown) dust and then settled out of the water column onto the substrate. This interpretation is based on the well-sorted, silt-sized character of the grains and the proximity of eolian environments along the paleocoastline (Budd and Loucks, 1981).

Thin-bedded carbonate mudstones are interpreted as mud-rich gravity flows because of the presence of traction features (Fig. 9C) and upward-fining sequences with elevated concentrations of quartz silt at the base of the flows. Additionally, both presence of early fracturing, bed-parallel slip, and injection of unlithified mud into early fractures in compacted carbonate beds, indicate that the substrate was unstable after deposition.

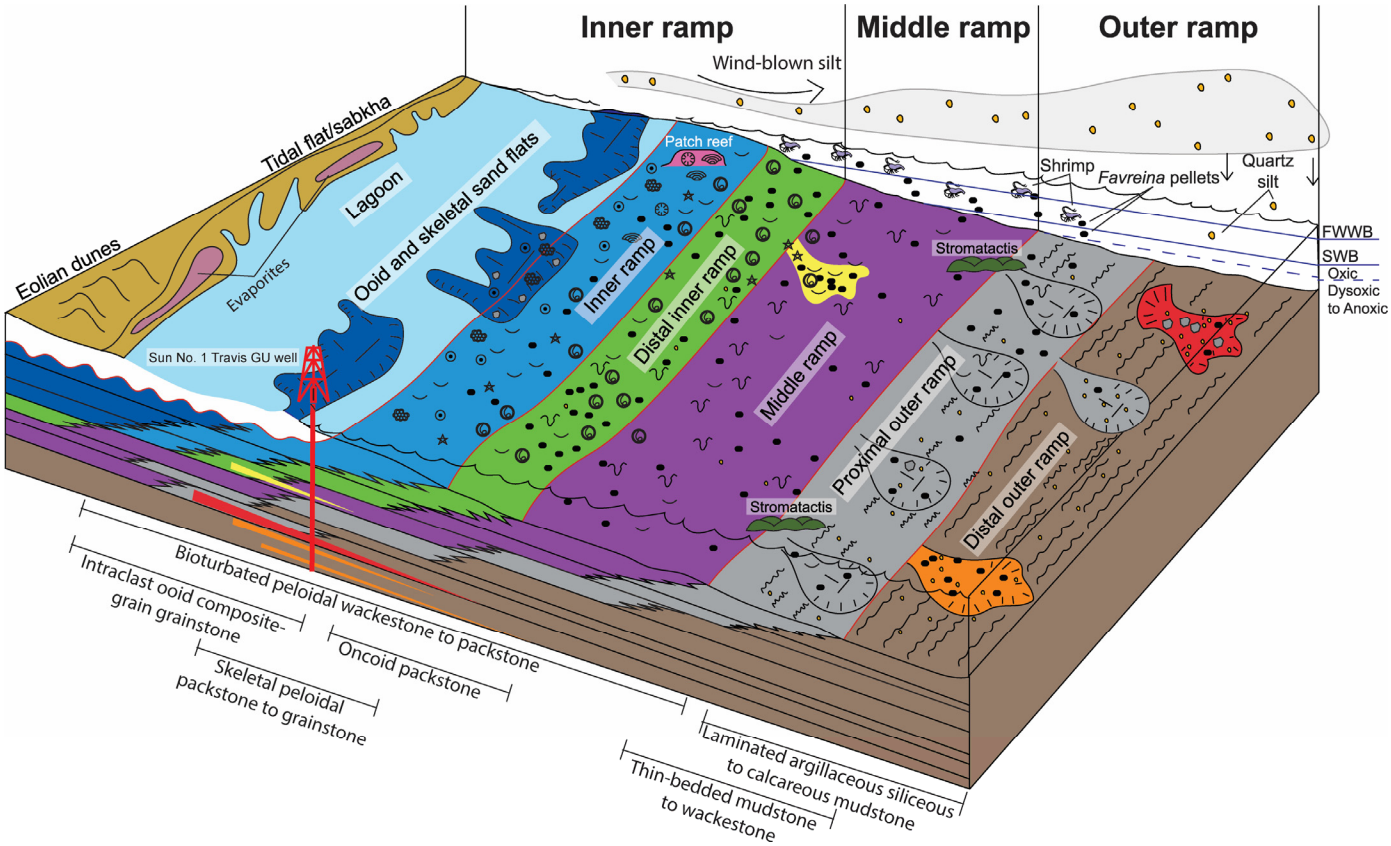

Figure 8. Smackover depositional model, northeastern Texas. See Figure 5 for legend.

Silty Peloidal Wackestone to Packstone

Description: This lithofacies is composed of *Favreina* pellets and quartz silt within a carbonate mud matrix (Fig. 10B). Beds are generally structureless or display upward-fining sequences and are 2 to 11.8 in (5 to 30 cm) thick with some beds that are 3.3 to 6.6 ft (1 to 2 m) thick. Most packages are composed of quartz silt (mud- to grain-supported), clay minerals, and peloids. Some beds have small amounts of bivalve fragments. The lithofacies is generally bounded above and below by dark argillaceous and silty dissolution seams.

Interpretation: Presence of coarser grains relative to the vertically adjacent lithofacies and upward-fining sequences suggests that the silty peloidal wackestone to packstone lithofacies was deposited by episodic mud-rich gravity flows that incorporated debris as they traveled down the ramp.

Granular- to Pebble-Sized Calcareous Breccia

Description: This lithofacies is made up of poorly-sorted angular clasts supported by a silty peloidal wackestone to packstone matrix (Fig. 10B). The intraclasts are composed of laminated mudstones, silty peloidal wackestone to packstone, and some eroded microbial-mat rip-up clasts (Figs. 10D and 10E). Below and above this lithofacies are abundant soft-sediment deformation and injection features.

Interpretation: This lithofacies is interpreted as debris-flow deposits, on the basis of abundant clasts supported by a carbonate mud matrix and the incorporation of other material during transport.

Thin-Bedded Mudstone to Wackestone

Description: This lithofacies is made up of thinly bedded mudstones to wackestones that are separated by wavy, organic-rich, silty argillaceous dissolution seams (Figs. 11A–11C). These mudstones to wackestones commonly contain upward-fining sequences and peloidal lags (Fig. 11B). The amount of peloids and skeletal fragments within the lithofacies increases upsection in the core. Additionally, there is an increase in soft-sediment deformation, abruptly truncated bioturbated intervals, and diagenetic alteration by dolomite and celestite upsection as well. Zones of dissolution seams (Figs. 11B and 11C) range in thickness from millimeters to tens of centimeters and are commonly surrounded by diagenetic alteration halos. These dissolution seams may be a combination of microbial mat and pressure solution. They contain high TOC, as much as 1.59 wt%, and some contain celestite crystals within the seam.

Interpretation: These thin beds are made up of stacked packages that contain traction and upward-fining sequences similar to the thin-bedded mudstones within the lower laminated mudstone interval. Stacking of these beds indicates multiple episodes in which these mud flows were deposited. The dissolution seams formed during intermediate (i.e., 1000 to 3000 ft [330 to 915 m]) burial depths. Concentrated insoluble material such as quartz silt, clay minerals, and organic matter likely accumulated during periods of low-energy waning currents. These seams form contacts between carbonate mudstone beds. Thickness of these seams may be related to the amount of time or the amount of insoluble material accumulated between mud-flow events.

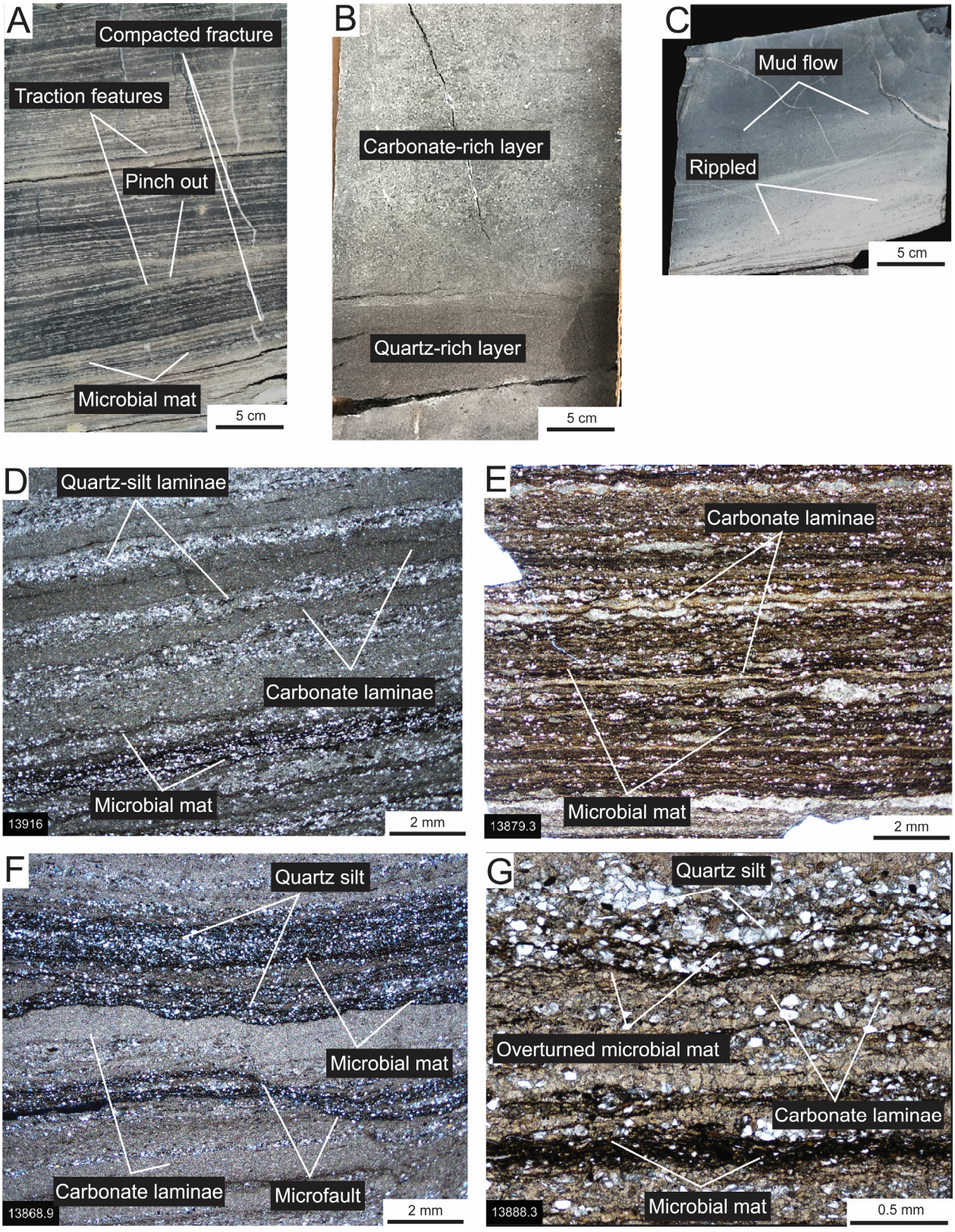

Figure 9. Lower Smackover lithofacies. (A) Laminae produced by bottom currents and microbial mats. Core photograph. (B) Silty peloidal packstone lithofacies, darker portion of the core contains more silt, and the lighter portion is more carbonate- and peloid-rich. Core photograph. (C) Thin-bedded argillaceous mudstone with ripples. Core photograph. (D) Interlaminated carbonate and quartz silt-rich laminae. Microbial mats form some of the laminae. Thin-section photomicrograph. (E) Interlaminated microbial mat and carbonate laminae. Wavy character related to irregular mats and compaction. Thin-section photomicrograph. (F) Interbedding of microbial mats, carbonate laminae, and silt-rich laminae. Soft-sediment microfault is present. Thin-section photomicrograph. (G) Interbedding of microbial mats, carbonate laminae, and silt-rich laminae. Microbial mat at base of quartz-rich silt layer is overturned indicating that the mat formed at the seafloor and is not a pressure solution seam. Thin-section photomicrograph.

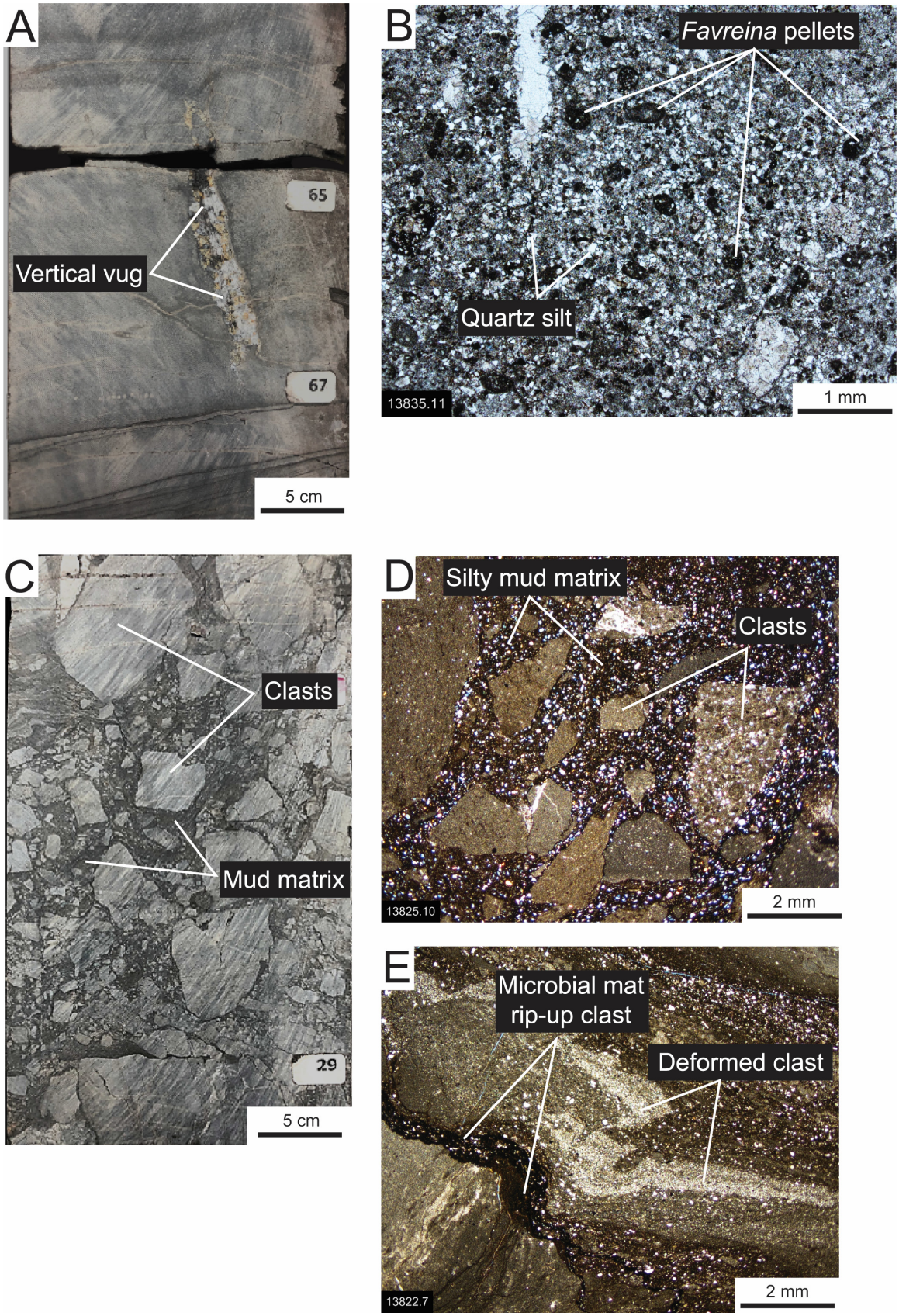

Figure 10. Lower Smackover lithofacies. (A) Open vug in the thin-bedded mudstone lithofacies partly occluded with dolomite and sulfide minerals. Core photograph. (B) Silty peloidal wackestone to packstone with *Favreina* pellets in quartz-silt-rich matrix. Thin-section photomicrograph. (C) Debrite with angular mud clasts in carbonate mud matrix. The mud clasts originated from very firm or semilithified carbonate mud. Striations on face of core are saw marks. Core photograph. (D) Mudstone to packstone clasts suspended in silty mud-rich matrix. Thin-section photomicrograph. (E) Deformed laminated mud clasts. Microbial rip-up clast present. Thin-section photomicrograph.

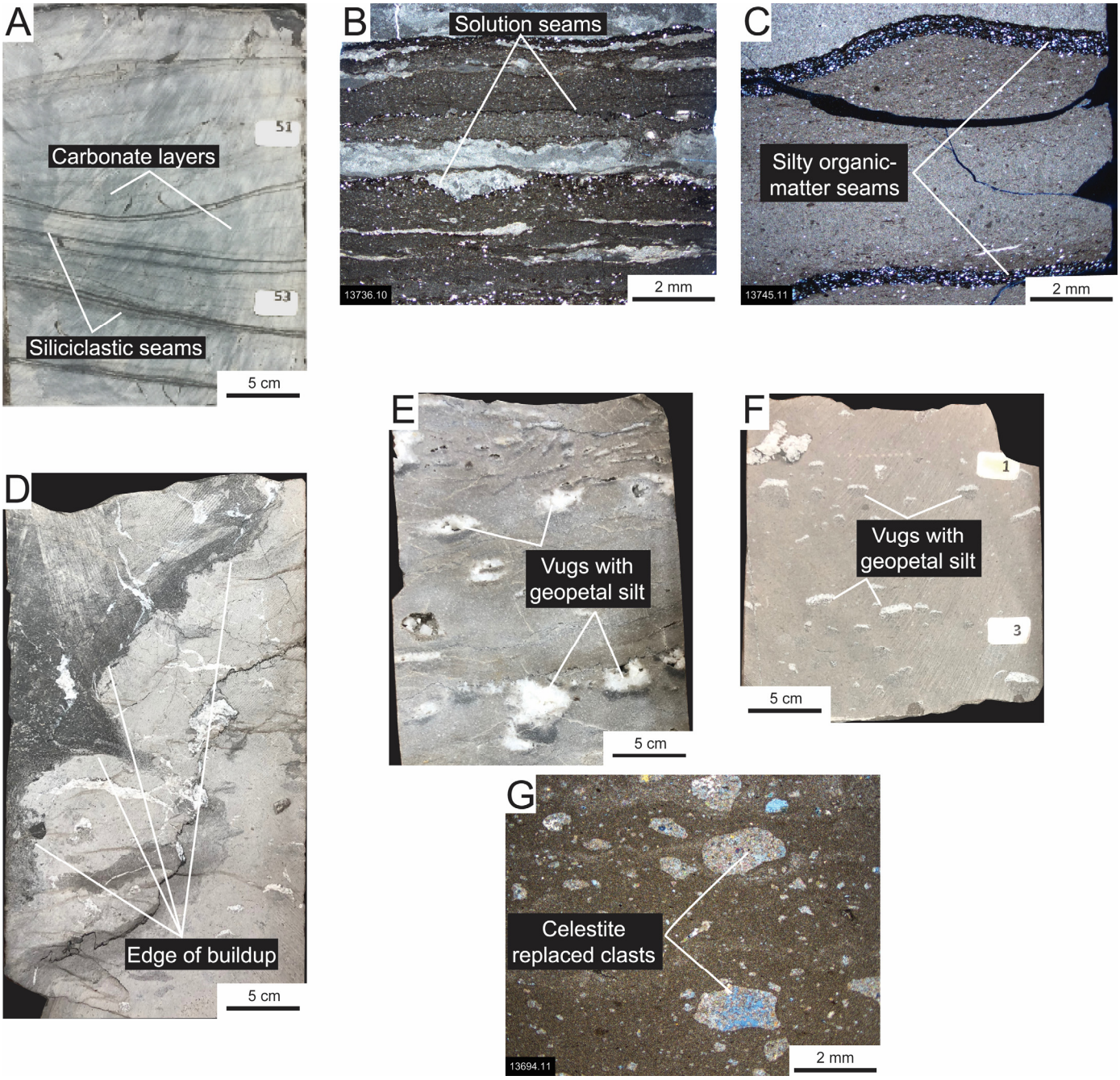

Figure 11. Lower Smackover lithofacies. (A) Laminated to thin-bedded mudstone to wackestone with silty organic seams. Core photograph. (B) Laminated silty mud with thin solution seam. Thin-section photomicrograph. (C) Silty peloidal mud with solution-enhanced seams of silty organic matter (microbial mats?). Thin-section photomicrograph. (D) Contact between stromatactis buildup and surrounding sediment. Core photograph. (E and F) Cavities (stromatactis) with geopetal silt and dolomite cement in top of cavity. Thin-section photomicrograph. (G) Eroded clasts replaced by dolomite and celestite (blue mineral). Thin-section photomicrograph.

Stromatactis Boundstone

Description: This lithofacies (Figs. 11 D–11G) is composed of a fabric that has been heavily altered by fine-crystalline dolomite. The fabric is mud-dominated with peloids supported by a finer mud matrix. It contains abundant, laterally elongated cavities with geopetal sediment at the base and the upper part of the cavity filled by coarse-crystalline equant dolomite (Figs. 11E and 11F). Some clasts are replaced by dolomite and celestite (Fig. 11G). Figure 11A shows what is interpreted as an angular contact between the buildup and the surrounding sediment. Along the contact are abundant intraclasts suspended within the lighter colored boundstone lithofacies.

Interpretation: There is some uncertainly in this lithofacies interpretation because of the diagenetic alteration and the cryptic rock fabric. The cavities resemble "stromatactis" structures that are commonly associated with mud mounds or thrombolites that are considered to have an organic or inorganic origin (Flügel, 2004, p. 194). Additionally, peloidal material incorporated with-

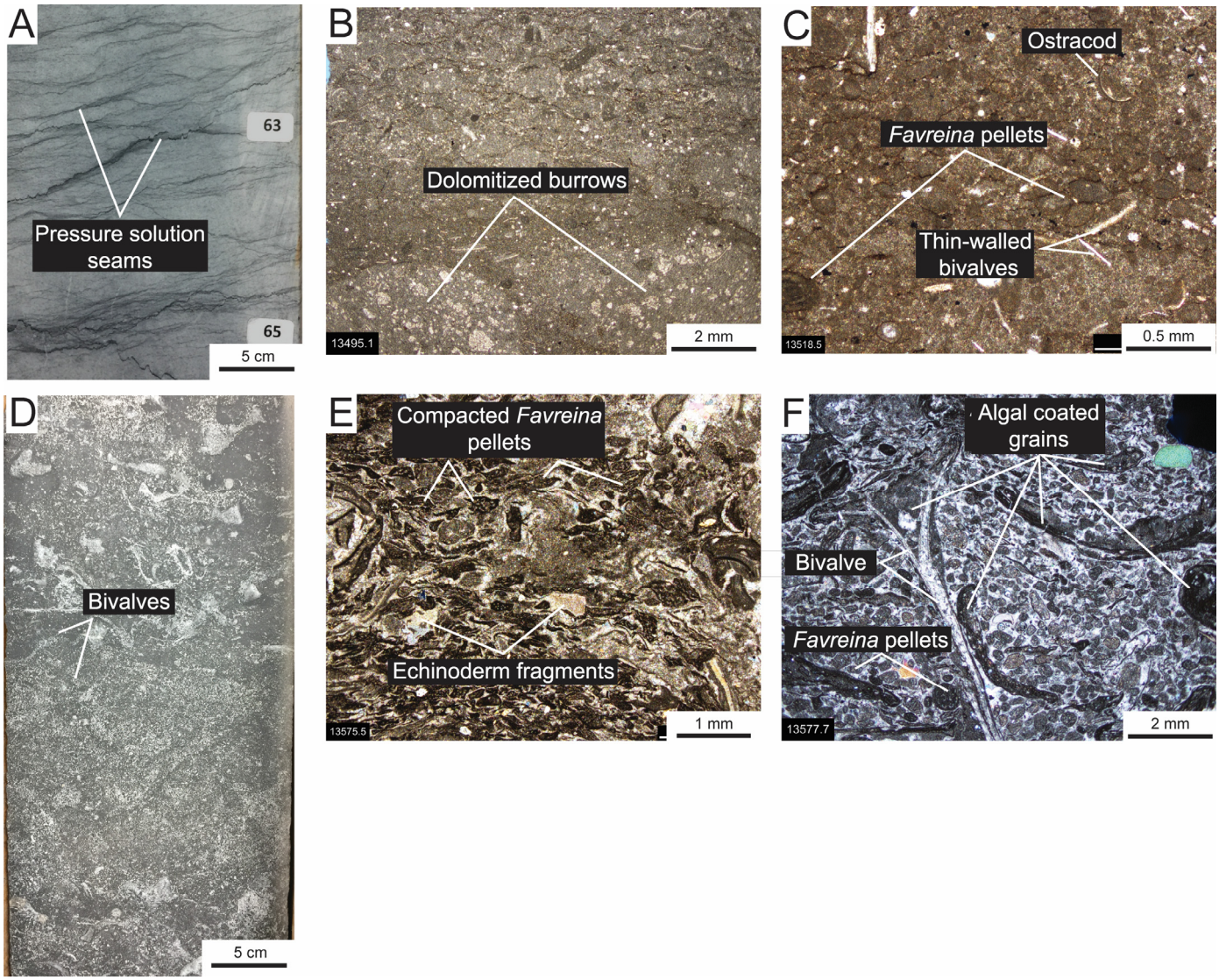

Figure 12. Middle Smackover lithofacies. (A) Bioturbated peloidal wackestone to packstone with abundant horse-tail dissolution seams. Core photograph. (B) Dolomitized burrows in a wackestone matrix. Thin-section photomicrograph. (C) Peloids and thin-walled bivalves within a carbonate mud matrix. Thin-section photomicrograph. (D) Highly bioturbated (i.e., massive) *Favreina* skeletal grainstone with large bivalves. Core photograph. (E) Abundant compacted *Favreina* pellets. (F) Grainstone with microbial coated grains and *Favreina* pellets.

in the mud-mound matrix and intraclasts at the edges of the mounds are commonly associated with stromatactis growth (Matyszkiewicz, 1993).

Middle Smackover Formation Lithofacies

Bioturbated Peloidal Wackestone to Packstone

Description: This lithofacies is composed of bioturbated wackestone to packstone containing abundant peloids, *Favreina* pellets, and skeletal fragments (Figs. 12A–12C). The skeletal material within the lithofacies is predominantly thin-walled bivalves, echinoderm fragments, and oyster fragments. Some algal-coated skeletal grains are also present and are most common upsection. Peloid grains and matrix material within burrows have been preferentially replaced by dolomite (Fig. 12B). The lithofacies also contains abundant clay-mineral-rich, horse-tail dissolution seams and stylolites (Fig. 12A). Firm grounds are also observed as abrupt boundaries commonly associated with rip-up clasts above or sediment-filled burrows below. These surfaces become more common upsection as the bioturbated lithofacies transitions into the oncoid packstone lithofacies.

Interpretation: On the basis of the abundance of mud and bioturbation, we interpret that this lithofacies reflects a low-energy, quiet-water setting with oxygenated bottom-sediment-water conditions. Oxygenated bottom waters allowed organisms to rework the sediment, and their skeletal remains and peloids contributed to the sediment mass. This interpretation is similar to those of Budd and Loucks (1981) and Harwood and Fontana (1983) of a similar lithofacies in South Texas and East Texas, respectively.

Favreina Skeletal Grainstone

Description: This lithofacies is composed of grain-rich intervals containing skeletal fragments and *Favreina* pellets (Fig. 12C). The grains include bivalves, echinoderms, and oyster fragments, most of which have thin microbial coatings (Fig. 12F).

The grains have undergone physical compaction resulting in broken skeletal material and compacted *Favreina* pellets (Fig. 12E). The grainstone intervals are interbedded with the bioturbated peloidal wackestone to packstone lithofacies separated by sharp dissolution seams or stylolitic contacts.

Interpretation: This lithofacies suggests gravity-flow deposition onto the middle ramp. Our interpretation is based on the abundance of shallow-water grains in a massive fabric located in the middle ramp section. Also, this lithofacies style sharply contrasts with depositional styles of the inner and outer ramp lithofacies.

Upper Smackover Formation Lithofacies

Oncoid Packstone

Description: The oncoid packstone lithofacies is composed of algae-coated (microbial) peloidal and skeletal grains (Figs. 13A–13C). The fabric is predominantly packstone and grainstone, but in some sections is floatstone and rudstone, depending on the size of the oncoids. Sizes vary from 0.012 in (0.3 mm) to more than 0.8 in (2 cm) in diameter, and the nucleus is commonly replaced by anhydrite (Fig. 13C). Texture is generally bimodal, with oncoid grains suspended in a dolomitized clotted peloidal packstone matrix with variable amounts of skeletal fragments (Fig. 13C). Skeletal grains are mainly thin-walled bivalves, echinoderm fragments, and oyster fragments. Most skeletal grains, including rip-up clasts and peloids, have some amount of algal coating (e.g., Fig. 13E).

Parts of the lithofacies contain cycles of firm grounds (possibly some are hardgrounds) with sediment-filled burrows, overlain by rip-up clasts and upward-fining sequences of older sediment (i.e., eroded from below the firm ground) (e.g., Fig. 13A). Other parts of the lithofacies have been heavily altered by fabric-destructive coarse-crystalline dolomite.

Interpretation: The lithofacies composed of oncoids indicates deposition in an environment within the photic zone having moderate-energy conditions that produce periodic agitation of grains. Periodic agitation was probably caused by storm-related currents or waves. The source of sediment in burrows below the firm grounds is related to transport of loose bottom sediment during high-energy-storm events.

Skeletal Peloidal Packstone and Grainstone

Description: The skeletal peloidal packstone to grainstone lithofacies is primarily composed of skeletal fragments and abundant peloids within a generally dolomitized matrix (Fig. 13D and 13F). Skeletal grains are bivalves, echinoderms (Fig. 13F), corals (Fig. 13F), and red algae (Fig. 13E); many grains have some algal coating (Fig. 13E). Some peloids are *Favreina* pellets. Most grains other than echinoderm and bivalve fragments have been heavily micritized. Multiple firm grounds overlain by rip-up clast are present. Some burrows are highly dolomitized.

Interpretation: This lithofacies is grain-rich but poorly sorted, and it was most likely deposited in a moderate- to high-energy setting within fair-weather wave base in an environment such as a sand flat. The variety of grain types indicates that the environment supported a diverse biota in well-oxygenated, normal-marine-salinity water.

Intraclast Ooid Composite-Grain Grainstone

Description: This lithofacies has been heavily altered by fabric-destructive dolomitization and micritization of grains, which makes it difficult to describe (Figs. 13H and 13I). The intense dolomitization is probably the result of evaporative brines sourced from the Buckner Anhydrite above. It is composed of intraclasts, micritized grapestones, ooids, and rhodoliths (Figs. 13H and 13I). The lithofacies contains intraclast-rich grainstones that fine upward into well-sorted, coarse-grained, grain-dominated packstones. Some intervals have faint cross laminae. The top of this lithofacies unit forms the contact between the Smackover Formation and the overlying Buckner Anhydrite. The contact is marked by a calichified erosional surface (Fig. 14A).

Interpretation: The combination of grain types in this lithofacies suggests a complex setting that evolved over time. The ooids and rhodoliths indicate periods of moderate- to high-energy conditions, and the composite grains (i.e., micritized grapestones) indicate periods of lower energy wherein grains could be bound together by cementation or by biological processes. Intense micritization process probably took place during lower energy conditions. Overall, the setting was of an energy level that did not preserve mud and varied in wave and current action, and as indicated by erosion-derived intraclasts, this lithofacies was affected by storm events.

Buckner Anhydrite Lithofacies

The Buckner section of the core (Fig. 14) is composed predominantly of anhydrite and interbedded sandstones. The anhydrite may have been originally anhydrite, or it may have been gypsum that transformed to anhydrite as a result of dehydration during burial. As gypsum changed to anhydrite, the volume decreased, which may have caused original depositional features to be altered, deformed, or completely obliterated (Mann and Kopaska-Merkel, 1992). Additionally, the Louann Salt was probably active during and after Buckner Anhydrite deposition, which led to tectonic deformation of the anhydrite units (Wilkinson, 1984). These factors may have obscured some of the depositional detail of the Buckner Anhydrite section.

Palmate Anhydrite

Description: The undisturbed to contorted beds of palmate anhydrite contain variable amounts of dolomite, quartz silt, and clay minerals filling between the anhydrite (Fig. 14B). Palmate crystals are smeared, squeezed, and offset from one another where the anhydrite is distorted (Fig. 14C). Even the best preserved palmate structures show signs of deformation, but their structure and size remain identifiable (Fig. 14B). The example of palmate anhydrite in Figure 14B has toppled onto its side. Palmate structures range from 0.8 to 2.8 in (2 to 7 cm) in height and have clear elongated lobe-shaped features with multiple orientations that may radiate from a single point. In the lower part of the Buckner Anhydrite section, the anhydrite is commonly deformed, but further upsection the anhydrite structures are better preserved. Intervals of palmate anhydrite are commonly separated or capped by mud drapes.

Interpretation: Formation of palmate structures is an indicator of subaqueous evaporite development. These palmate structures commonly grew into subvertical bushes of palm-frond-shaped crystals on the sediment surface in shallow, subaqueous hypersaline environments (i.e., salinas) (Schreiber et al., 1977, 1982; Loucks and Longman, 1982).

Fine-Nodular Anhydrite

Description: This lithofacies is composed of thin-bedded, moderately- to well-sorted anhydrite nodules generally within a sandstone or mudstone matrix (Figs. 14C and 14E). Some of the anhydrite nodules may actually be eroded and transported clasts (Figs. 14D and 14E). The beds commonly occur at the base of anhydrite-cemented sandstone lithofacies and have upward-fining grading.

Interpretation: Several interpretations of the anhydrite nodules are presented. The nodules are well sorted, angular to rounded, and commonly are concentrated at the base of sandstone packages, which indicates that they may have been eroded and

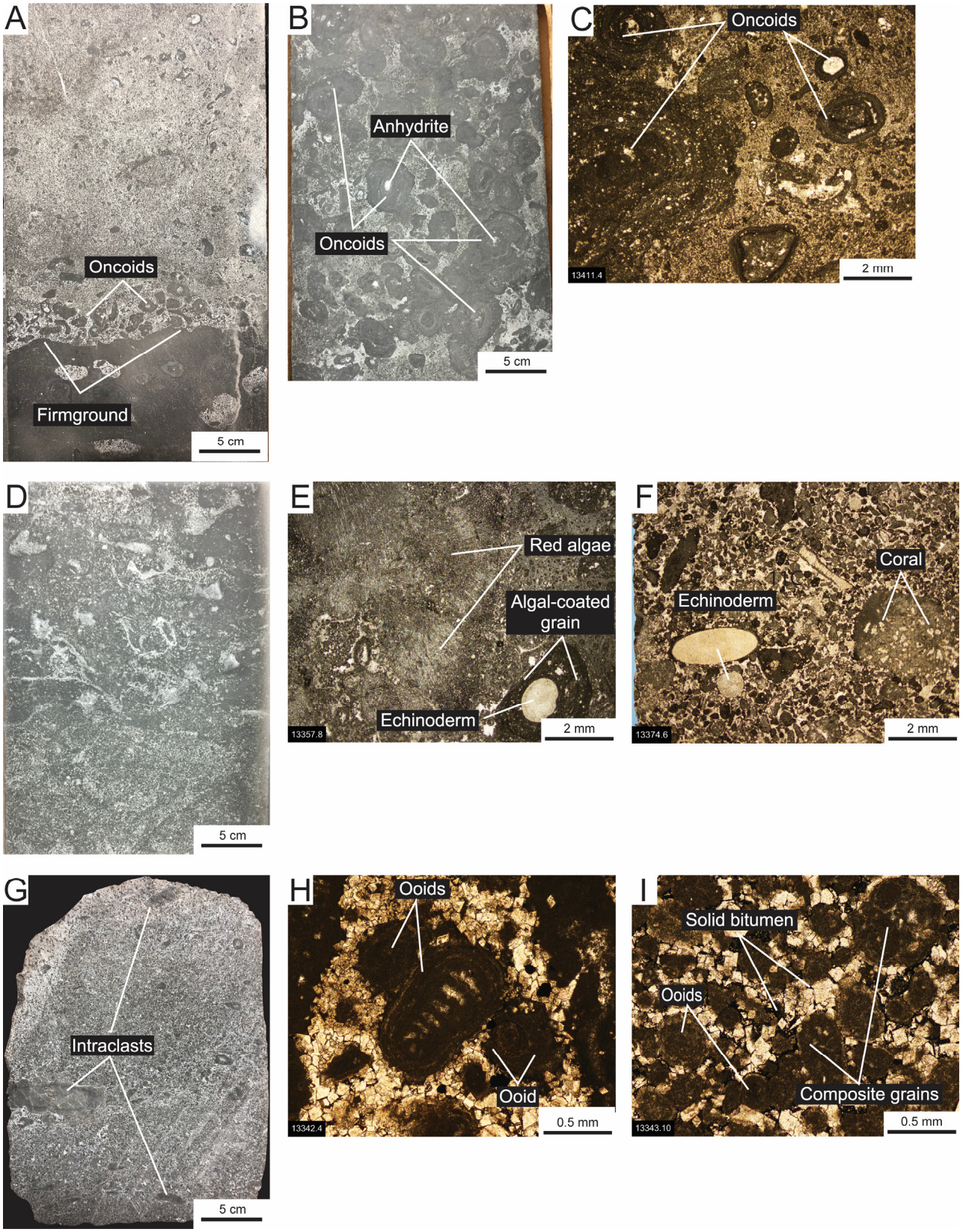

Figure 13. Upper Smackover lithofacies. (A) Firm ground with sediment filled burrows, overlain by rip-up clasts and an upward-fining sequence. Core photograph. (B) Oncolite rudstone with anhydrite replacing some nuclei. Core photograph. (C) Oncoids in a dolomitized mud matrix. Thin-section photomicrograph. (D) Skeletal peloidal packstone to grainstone with large skeletal fragments. Core photograph. (E) Packstone containing fragments of red algae and echinoderms. Echinoderm fragment is microbially coated. Thin-section photomicrograph. (F) Grainstone with coral, echinoderms, *Favreina* pellets, and peloids. Interparticle pore space filled by dolomite. Thin-section photomicrograph. (G) Intraclast ooid composite-grain grainstone with intraclasts. Core photograph. (H) Ooid grainstone with dolomite pore fill. Ooids are highly micritized. Thin-section photomicrograph. (I) Ooid grainstone with interparticle pores filled with dolomite and solid bitumen. Thin-section photomicrograph.

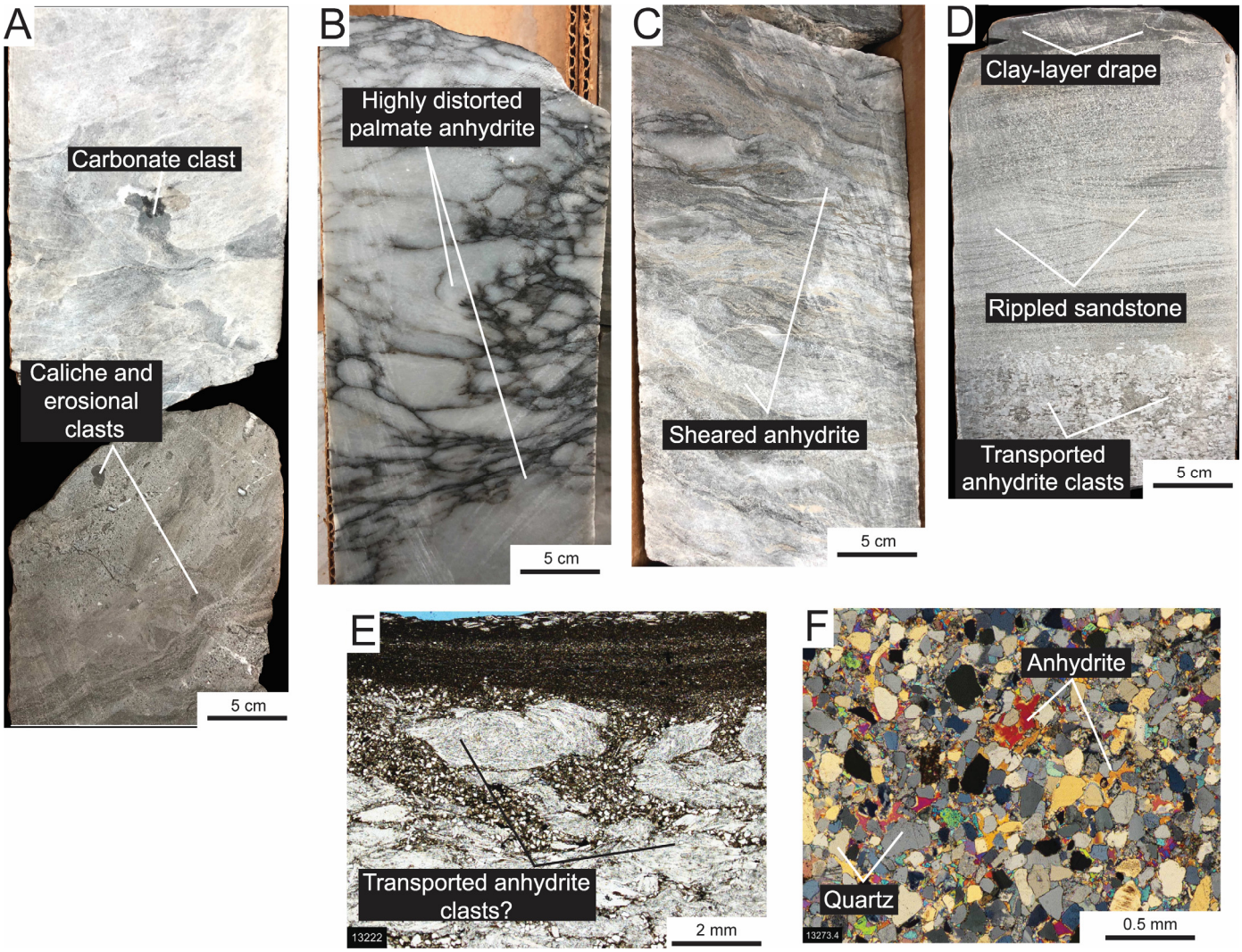

Figure 14. Buckner Anhydrite lithofacies. (A) Contact between Smackover Formation and Buckner Anhydrite (a few inches is missing between the two core pieces). Top of the Smackover Formation is eroded, and caliche formed on the surface before Buckner Anhydrite was deposited. Caliche displays soil-related deformation and contains crusts and transported gravel. The massive anhydrite above may be highly deformed palmate anhydrite. Core photograph. (B) Highly distorted palmate crystals highlighted by dark seams. Core photograph. (C) Sheared anhydrite with streaks of quartz silt. Core photograph. (D) Multiple depositional events consisting of transported small anhydrite clasts at base with rippled sandstone above. Sandstone capped by clay-layer drape. Core photograph. (E) Transported anhydrite clasts in a silty mud matrix. Thin-section photomicrograph. (F) Coarse silt to very fine quartz sandstone cemented by anhydrite. Thin-section photomicrograph under cross-polarized light.

transported as clasts. This is likely the case where the lithofacies is below the anhydrite-cemented sandstone lithofacies. Alternatively, the nodular anhydrite may form by in-situ growth within a sabkha setting.

Laminated Anhydrite

Description: The laminated anhydrite facies is interbedded with several other lithologies, including dolomite-rich anhydrite, clay-mineral drapes, medium-sized isolated anhydrite nodules, small, bedded anhydrite nodules, and some thin layers of sandstone.

Interpretation: Laminated evaporites generally form in subaqueous stagnant conditions, typical of salina or salt-pan settings (Warren, 2006, p. 23). The associated siliciclastic sediment is commonly windblown in origin. Isolated anhydrite nodules may be original or recrystallized from the laminated evaporites.

Anhydrite-Cemented Sandstone

Description: The anhydrite-cemented sandstone is composed of fine-grained quartz-rich sand that are well sorted and generally cemented with anhydrite (Fig. 14 F). These sandstones are mostly massive, but some ripples and crossbeds are preserved (Fig. 14D). Sandstone packages are commonly capped by mud drapes (Fig. 14D) and large displacive anhydrite nodules are observable within upper sections of the sandstone packages.

Interpretation: The sandstone packages represent fluvial sedimentation events that were probably the result of slightly wetter periods of time within the wadi environment. As mentioned above, the eroded fine-nodular-anhydrite lithofacies is commonly present at the base of the sandstones and likely constitutes the basal part of the flows that deposited the sands.

Interbedded Sandstone and Anhydrite

Description: This lithofacies is composed of alternating thin beds of sandstone and nodular anhydrite; sandstone proportions increase vertically. The lithofacies lacks sedimentary structures within beds.

Interpretation: This lithofacies may indicate periods of sustained subaerial exposure where wadi/eolian processes depositing sand dominated. The anhydrite may have displacively formed within the sediment in response to variations in sediment-water saturation related to periodic flooding (wadi processes) and subsequent sand deposition (eolian processes) (Warren, 2006, p. 40).

Siliciclastic-Rich Mudstone

Description: The siliciclastic-dominated mudstone lithofacies is composed of dark nonfossiliferous mudstone interbedded with anhydrite clasts. The mudstone shows faint laminations (Fig. 14). Anhydrite clasts are elongated to bedding and show some upward-fining sequences.

Interpretation: These siliciclastic mudstones indicate deposition from waning flows (e.g., storms). The anhydrite clasts appear to be eroded and transported. The laminated mudstone may be suspension deposition at the end of the waning flow. This process could be related to episodic wadi flow, in which the wadi cut into previously deposited evaporites.

SMACKOVER AND BUCKNER DEPOSITIONAL MODEL

The lower Smackover is composed of the initial marine carbonate sediments deposited in the East Texas Basin during the early stages of platform development; therefore, deposition in a ramp setting over the Norphlet topography would be expected as no continental shelf had been earlier established (Ahr, 1973; Ewing, 2001). The depositional model of the Smackover Formation along the Gulf of Mexico proposed by several authors is based on a carbonate ramp (e.g., Ahr, 1973; Budd and Loucks, 1981; Ewing, 2001; Heydari and Baria, 2005). Carbonate ramps gently dip seaward, and facies belts are generally parallel to the shoreline. Depositional processes are related to fair-weather and storm-wave base; however, local depositional processes can be affected by antecedent topography (Flügel, 2004, p. 665). The actual depth of fair-weather and storm-wave base varies in relation to local hydrodynamic/climatic conditions and with time (Burchette and Wright, 1992). Given the depths to fair-weather wave base and storm-wave base along the western shelf of Florida (Reading and Collinson, 1996) one might estimate that the depth to fair-weather wave base was likely in the range of 150 ft (~30 m), and storm wave base was in the range of 300 ft (~100 m). Above storm-wave base, lithofacies attributes are generally controlled by surface waves, tidal currents, storm processes, biological processes, and chemical processes, whereas below storm-wave base, lithofacies attributes are generally controlled by gravity-flow processes, biological processes, salinity-stratified water columns, oxygenation levels, and bottom currents.

Our Smackover-ramp depositional model is presented in Figure 8. Lithofacies present within the Sun No. 1 Travis Gas Unit core are referenced to this model based on sediment characteristics and interpreted associated physical and chemical processes. The ramp is subdivided into inner, middle, and outer ramps, which correspond to the upper Smackover, middle Smackover, and lower Smackover, respectively. The Buckner Anhydrite lithofacies are not referenced in this model because there is a break in deposition between the Smackover and Buckner Anhydrite sections.

The Smackover–Buckner Anhydrite section was deposited during approximately 8 million yr. Assuming that third-order sequences range from 0.5 to 5 million yr (Van Wagoner et al., 1990), one must assume that the area was subjected to several eustatic sea-level changes and that these changes would affect lithofacies stacking patterns. Indications of abrupt changes in lithofacies stacking patterns may be evidence of cycle changes within the described section. However, the area of this study was likely impacted to some degree by active salt movement, and the topography associated with salt movement may have affected lithofacies stacking patterns. Heydari and Baria (2005) discussed the progradational character of the Smackover Formation and noted forced regressions within the system. They reported that seismic data documented a clinoform architecture in parts of the system. Our investigation also recognizes several apparent forced regressions in the lower Smackover interval based on abrupt changes in stacking patterns (i.e., abrupt change from deeper water lithofacies to slightly shallower water [still deep] lithofacies). These forced regressions could be related to eustatic sea-level changes or to salt movement.

Lower Smackover Depositional Systems, Facies Tracts, and Lithofacies Stacking Patterns

In our depositional model (Fig. 8), the outer ramp is divided into two subsettings: distal outer ramp and proximal outer ramp. The distal outer ramp is characterized by low-energy dysoxic to anoxic sedimentation punctuated by gravity-flow deposits, all of which are interpreted to having been deposited below storm-wave base. The proximal outer ramp is similar to the distal outer ramp, but gravity-flow deposits are more prevalent, and stromatactis mounds are present (Fig. 8). Oxygenation levels may have increased near the updip boundary with the middle ramp.

Laminated mudstones of the lower Smackover section were deposited on the distal part of the carbonate ramp (Fig. 8) in anoxic bottom water. The climate during Smackover deposition was arid, and it supported evaporative conditions that resulted in a landward increase in salinity (Heydari and Moore, 1994). Additionally, positive features such as the Angeline Caldwell Flexure (Fig. 2) may have restricted circulation of sea water between the East Texas Basin and the more open Gulf of Mexico (Wood and Walper, 1974; Moore et al., 1988). These conditions likely led to elevated salinities within the East Texas Basin and potentially produced a stratified water column. A paleogeographic map of the Oxfordian (148.4 Ma) by Scotese (2014) that shows the paleo-Gulf of Mexico as a restricted interior basin between South America and North America adds additional evidence that the Smackover sediments were deposited in a semi-restricted setting, which likely contributed to anoxic bottom-water conditions.

High salinities and low oxygen content within sea water restrict biodiversity in marine environments (Oschmann, 1993). This environmental stress may explain the presence of microbial features such as sulfur-reducing microbial mats preserved in lower Smackover strata. Microbial organisms are resilient and thrive in stressed environments because these environments restrict metazoan grazers (Mancini et al., 2004; Schieber et al., 2007). Grazers inhibit microbial growth and quickly outcompete microbial organisms for territory (Schieber et al., 2007). In the anoxic and high-salinity environment in which the lower Smackover sediments were deposited, microbial mats developed periodically and were likely a dominant contributor of organic matter to lower Smackover source rocks.

The laminated mudstones contain carbonate-rich laminae alternating with quartz-silt and organic-rich laminae. This feature has several possible explanations. The first is that organic-rich microbial-mat growth was interrupted by brief sedimentation events such as hemipelagic mud plumes or whitings that supplied carbonate mud to distal environments through suspension settling. Muds in the outer-ramp setting may have also been partly sourced by planktic coccolithophores that lived in open-marine waters within the photic zone. However, no coccolith material

was observed in our scanning electron microscope analysis, and these planktonic organisms have not been mentioned within previous Smackover literature. But because of the higher maturity level (calculated R_o = 1.1 or higher) seen in the investigated core, these organisms may have been obscured by diagenesis (i.e., cementation).

An alternative explanation of the fine-scale alternation in laminae lithologies is that the carbonate formed through in-situ precipitation in the microbial-mat laminae. Given suitable water chemistry, syngenetic carbonate precipitation in microbial mats can take place (Thompson and Ferris, 1990; Pratt, 2001; Schieber et al., 2007). This may have been a response to changing bottom-water chemistry toward more alkaline waters (Thompson and Ferris, 1990; Pratt, 2001).

The thin-bedded mudstones within the laminated mudstone lithofacies were probably deposited by dilute turbidity currents forming muddy turbidites in a similar process that resulted in the deposition of the silty peloidal wackestone to packstone lithofacies. These gravity-flow deposits appear to be more mud-dominated in distal environments and as shallower water Smackover lithofacies prograde into the basin, gravity-flow deposits became more peloidal and skeletal-rich. The core description in Figure 4 shows cycles, discernable by the bundling of mud-rich debrites, which may be controlled by fourth-order sea-level cycles. There appears to be a cycle top in the middle of the laminated lithofacies (13,883 ft [4231.5 m]) and a second cycle at the top of the lithofacies (approximately 13,820 ft [4212.3 m]) as it transitions to the silty peloidal wackestone to packstone lithofacies and is finally capped by the granular to pebble calcareous breccia lithofacies (debrite). The presence of rip-up clasts of underlying sediment within the debrite indicates that some gravity flows were erosive. Debrites, early fracturing, and tilting of beds may indicate that the Smackover ramp was at times unstable, suggesting that these features may have been triggered by early instability of the ramp as a result of the migration of underlying salt (Wilkinson, 1984).

Following the debrite lithofacies below there is a transition into thin-bedded mudstone to wackestone lithofacies, interpreted as stacked mud-rich debrites. The shift toward higher concentrations of flow deposits indicates increasing carbonate sediment being transported down the ramp and suggests a more proximal depositional environment than that associated with a greater proportion of laminated mudstones, or it may indicate an increase in the amount of sediment being produced. In either case, the increased sedimentation probably inhibited microbial-mat growth. These thin-bedded mudstones are interbedded with the laminated mudstones, bioturbated mudstones, and stromatactis boundstone buildups. Changes between lithofacies can be attributed to several factors, including variations in depth, sedimentation rate, or the position in the water column of the anoxic bottom-water layer. These variations may all be linked and controlled by fourth-order sea-level cycles. The thin-bedded mudstones are a transitional lithofacies between the outer ramp and the middle ramp. The mudstones show an increasing skeletal content upsection, indicating an increase in the amount of sediments from shallower environments being transported by gravity-flow currents. Additionally, interbedding with bioturbated lithofacies becomes more common upsection as well, suggesting proximity to oxygenated waters. These observations point toward the lithofacies representing shallowing but still relatively deep conditions, or an increasing proximity to oxygenated waters.

The stromatactis boundstone lithofacies is relatively nondescript except for the distinct geopetal-filled cavities and remnant growth structures. The matrix of this lithofacies is massively dolomitized such that the fine-scale matrix features are obliterated. Flügel (2004, p. 196) described a variety of paleoenvironmental settings of stromatactis-rich rocks. In general, this stromatactis boundstone lithofacies is associated with low-energy, moderate-water depths ranging from above to below storm-wave base. Additionally, they have been known to form at the flanks of sediment buildups, such as debrites, in ramp settings (Flügel, 2004, p. 196). This environmental interpretation agrees with the middle- to outer-ramp position of stromatactis in our model.

Middle Smackover Depositional Systems, Facies Tracts, and Lithofacies Stacking Patterns

The middle-ramp setting (Fig. 8) is characterized by oxygenated bottom-water and sediment conditions and low-energy deposition, where mainly muddy sediments accumulated (Fig. 8). The outer part of the middle ramp was below storm-wave base and the inner part was above storm-wave base, but still below fair-weather wave base. This setting had oxic conditions that promoted an increase in biota. Some grain-rich gravity-flow deposits, sourced from the inner ramp, were transported onto the middle ramp. These conditions were likely present along a large portion of the Smackover ramp, as indicated by the abundance of the bioturbated peloidal wackestone to packstone lithofacies. The thickness and areal extent of the lithofacies were probably determined by the paleoposition of the storm-wave base, the anoxic bottom-water layer, and the slope of the ramp.

Bioturbated peloidal wackestone to packstone is the most common lithofacies within the middle ramp (Figs. 4 and 8), and it is the primary lithofacies that composes the middle Smackover Formation (from approximately 13,602 ft [4145.9 m] to13,473 ft [4106.8 m]). Bioturbation obscured hydrodynamic sedimentary features, making it difficult to interpret depositional processes. Mud in this interval was probably transported into the environment by hemipelagic plumes, long-shore currents, or by gravity-flow currents from updip shallower ramp environments (Burchette and Wright, 1992). Skeletal and algal-coated grains such as those in the *Favreina* skeletal grainstone lithofacies were probably sourced from the updip shallower ramp related to storm-induced flows (Burchette and Wright, 1992). Biota in this oxygenated setting consumed organic matter as it was deposited, leading to its low preservation in the rock record. There is an increase in bioturbation, skeletal grains, and peloid types and size upward in the section, suggesting increasingly favorable living conditions for organisms and, as a result, greater biodiversity. This biodiversity may be related to an increased supply of oxygen at the sediment-water interface as the depositional setting became shallower.

Upper Smackover Depositional Systems, Facies Tracts, and Lithofacies Stacking Patterns

The inner ramp is divided into two subsettings (Fig. 8): a distal inner ramp and a broad proximal inner ramp. The entire inner-ramp setting was well oxygenated within fair-weather-wave base; a broad range of energy levels is evidenced by a variety of mud- to grain-dominated facies. Some areas of elevated salinities in the inner ramp potentially produced sea-water supersaturated relative to aragonite, and this condition favored ooid production (Moore et al., 1988; Heydari and Moore, 1994).

Although the upper Smackover lithofacies are heavily altered by fabric destructive dolomitization (e.g., Fig. 13I), depositional fabric and texture can still be discerned. The inner-ramp lithofacies evolved from the oncoid packstone lithofacies through the skeletal peloidal packstone to grainstone lithofacies to the intraclast ooid/composite-grain grainstone lithofacies, producing an overall upward decrease in carbonate mud, an increase in grainier lithofacies, and an increase in sorting, all of which suggest shoaling upward into a shallower-water, higher-energy depositional setting. Additionally, the abundance of firm grounds and upward-fining sequences through the three lithofacies indicates a number of episodic depositional events of sedimentation that may be related to effects of large storms (Wanless et al., 1988).

The depositional characteristics of these lithofacies indicate higher wave energy, which affected the sediments through the creation of complex nearshore facies mosaics (barrier bars, tidal channels, splays, etc., all with individual depositional architectures) (Flügel, 2004, p. 665). Adding to this complexity were topographic lows and highs formed by salt withdrawal and associated buildups in response to penecontemporaneous active salt movement (Jackson, 1982; Wilkinson, 1984) The oncoid packstone lithofacies is considered a transitional facies just below and within fair-weather-wave base, where bottom sediments were affected periodically by storm processes (Flügel, 2004, p. 136). Variations in the lithofacies and oncoid sizes indicate changes in energy and periodicity of agitation that controlled bottom conditions and associated oncoid growth. The skeletal peloidal packstone to grainstone lithofacies were deposited in moderate- to high-energy conditions above fair-weather-wave base. The presence of coral fragments and red algae within the grainstones may indicate nearby biohermal or biostromal development, although in situ structures are absent in this core. Occurrences of these grain types as well as various peloid types indicate normal-marine salinities and good living conditions overall.

The intraclasts and ooid composite-grain grainstone lithofacies is heavily dolomitized, but well-sorted intraclasts and coated grains can be easily distinguished. It contains fewer skeletal organisms than the underlying grainstone lithofacies and may suggest elevated salinities in a more restricted interior setting and moderate-energy conditions. Lithofacies indicating extensive shoal complexes are not clearly discernable within the investigated core. The intraclast ooid composite-grain grainstone lithofacies may be a subfacies of a former shoal complex, but if a thick section of ooids was deposited, the ooids eroded before the deposition of the overlying Buckner Anhydrite. The contact with the overlying Buckner Anhydrite is calichified. Truncation of the upper Smackover section and evidence of exposure suggest that the Buckner Anhydrite is in unconformable contact with the Smackover Formation and that strata eroded from the top of the Smackover Formation.

Buckner Anhydrite Depositional Systems, Facies Tracts, and Lithofacies Stacking Patterns

The depositional model in Figure 8 does not address the Buckner Anhydrite lithofacies. The Buckner Anhydrite is considered to be a part of a depositional sequence separate from the Smackover Formation (e.g., Wade and Moore, 1993). Therefore, deposition was not continuous between the two units.

The Buckner Anhydrite section of the core is challenging to interpret because of diagenetic distortion of features and the lack of well-recognized siliciclastic and carbonate depositional fabrics. However, the large amount of evaporites and development of palmate and laminated anhydrites indicates deposition in a subaqueous salina or salt-panlike setting to probable sabkhas (Loucks and Longman, 1982). Additionally, the abundance of well-sorted, fine-grained sandstones indicates eolian or wadi depositional processes. The low amount of carbonate material in the section suggests either a proximity to terrestrial depositional environments or a water chemistry unfavorable for carbonate precipitation. Also, given the very low angle of the ramp, the depositional setting may have been some distance landward from the open-marine carbonate factory. The anhydrite intervals represent subaqueous-evaporite development, whereas the sandy intervals probably result from either episodic subaqueous sediment depositional events or periods of subaerial exposure. Exposure may have taken place as a result of minor sea-level changes or movement of underlying salt structures or climate variations. During subaerial exposure, layers of anhydrite nodules may have developed at the saline water table, diagenetically emplacing nodules within the sand (Warren, 2006, p. 40).

CONCLUSIONS

The long continuous core from the Sun No. 1 Travis Gas Unit in Van Zandt County, Texas, is suggested as the type-cored section for the Smackover Formation and Buckner Anhydrite interval in northeastern Texas. This core contains most of the common lithofacies recognized from many other Smackover Formation and Buckner Anhydrite studies of the Gulf of Mexico area (e.g., Budd and Loucks, 1981; Ewing, 2001; Heydari and Baria, 2005).

In the study area the Smackover Formation has three subunits: lower, middle, and upper. Smackover strata were deposited on a low-angle ramp that extended along the northern Gulf of Mexico rim during Oxfordian time. The lower Smackover section was deposited in a deeper water (below storm-wave base), outer-ramp setting characterized by low-energy dysoxic to anoxic mud-dominated sedimentation punctuated by gravity-flow deposits. Predominant lithofacies are laminated argillaceous to calcareous mudstones and wackestones with some granular- to pebble-sized calcareous conglomerates and stromatactis boundstone. Anoxically deposited microbial mats are associated with the laminated mudstones.

The middle Smackover section was also deposited in deeper water, but in a middle-ramp setting. This setting was characterized by low-energy, oxic conditions in which mainly muddy sediments accumulated. The outer part of the middle ramp was below storm-wave base, and the inner part was above storm-wave base but still below fair-weather wave base. The abundance of biota greatly increased in the middle-ramp interval in comparison to the outer-ramp interval of the lower Smackover section. Bioturbated peloidal wackestone to packstone is the predominant lithofacies deposited in this area; in this facies, the extensive bioturbation likely reflects an increase in quality of living conditions in the middle ramp, compared to conditions in the outer ramp.

The inner ramp is a complex mosaic of lithofacies deposited in low- to high-energy, oxic, and relatively shallow-water settings. Evidence of wave, tidal-current, and storm processes, such as oncoid and ooid development and crossbedding, is abundant. The complete section is interpreted as having been deposited within the fair-weather wave zone.

The Buckner Anhydrite section overlying the Smackover section is dominated by evaporites. Its depositional setting varied between sabkha and salina deposition. Palmate and laminated anhydrite lithofacies indicate subaqueous precipitation of evaporites (e.g., salina), whereas the nodular anhydrite suggests precipitation in a sabkha setting. Intermixed evaporites and siliciclastics indicate a mixed environment where several processes (submarine and terrestrial) intercalated the two lithofacies end members.

Our detailed lithofacies description of this type-cored section will aid in describing and interpreting other Smackover Formation and Buckner Anhydrite cores in northeastern Texas. The Sun Oil No. 1 Travis Gas Unit well will be useful in integrating and comparing the extensively drilled and studied Smackover Formation to the east with the relatively undrilled and lesser studied Smackover Formation in South Texas and along the east coast of Mexico.

ACKNOWLEDGMENTS

We want to recognize the Carbonate Reservoir Characterization Research Laboratory (RCRL) and the State of Texas Advanced Reservoir Research (STARR) program of the Bureau of Economic Geology at The University of Texas at Austin for major support of this investigation. We appreciate reviews of the manuscript by Kelly Hattori and David Hull. Amanda R. Masterson copy-edited a version of this manuscript. We also recognize Charles Kerans and Laura Zahm, who served on Peter Schem-

per's M.S. committee, from which this paper is in part derived. Publication authorized by the Director, Bureau of Economic Geology, Jackson School of Geosciences, University of Texas at Austin.

REFERENCES CITED

Ahr, W. M., 1973, The carbonate ramp; an alternative to the shelf model: Gulf Coast Association of Geological Societies Transactions, v. 23, p. 221–225.

Arthur, M. S., and B. Sageman, 1994, Marine black shales: Depositional mechanisms and environments of ancient deposits: Annual Review of Earth and Planetary Sciences, v. 22, p. 499–551.

Barnaby, R. J., 2013, Sedimentology and stratigraphy of lower Smackover tight oil carbonates: Key to predictive understanding of reservoir quality and distribution: 2013 American Association of Petroleum Geologists Black Shale Core Workshop, Pittsburgh, Pennsylvania, 19 May 2013, 23 p., <http://www.digitalstratigraphy.com/uploads/2/6/3/4/26341429/aapg_core_workshop_2013_presentation.pdf>.

Budd, D. A., and R. G. Loucks, 1981, Smackover and lower Buckner Formations, South Texas: Depositional systems on a Jurassic carbonate ramp: Bureau of Economic Geology Report of Investigations 112, Austin, Texas, 42 p.

Burchette, T. P., and V. P. Wright, 1992, Carbonate ramp depositional systems: Sedimentary Geology, v. 79, p. 3–57, <https://doi.org/10.1016/0037-0738(92)90003-A>.

Claypool, G. E., and E. A. Mancini, 1989, Geochemical relationships of petroleum in Mesozoic reservoirs to carbonate source rocks of Jurassic Smackover Formation, southwestern Alabama: American Association of Petroleum Geologists Bulletin, v. 73, p. 904–924, <https://doi.org/10.1306/44B4A28F-170A-11D7-8645000102C1865D>.

Dickinson, K. A., 1968, Upper Jurassic stratigraphy of some adjacent parts of Texas, Louisiana, and Arkansas: U.S. Geological Survey Professional Paper 594–E, p. E1–E25.

Dickinson, K. A., 1969, Upper Jurassic carbonate rocks in northeastern Texas and adjoining parts of Arkansas and Louisiana: Gulf Coast Association of Geological Societies Transactions, v. 19, p. 175–187.

Dunham, R. J., 1962, Classification of carbonate rocks according to depositional texture, *in* W. E. Ham, ed., Classification of carbonate rocks —A symposium: American Association of Petroleum Geologists Memoir 1, Tulsa, Oklahoma, p. 108–121.

Ewing, T. E., 2001, Review of Late Jurassic depositional systems and potential hydrocarbon plays of the northern Gulf of Mexico Basin: Gulf Coast Association of Geological Societies Transactions, v. 51, p. 85–96.

Ewing, T. E., 2009, The ups and downs of the Sabine Uplift and the northern Gulf of Mexico Basin: Jurassic basement blocks, Cretaceous thermal uplifts, and Cenozoic flexure: Gulf Coast Association of Geological Societies Transactions, v. 59, p. 253–269.

Flügel, E., 2004, Microfacies of carbonate rocks: Analysis, interpretation and application: Springer, Berlin, Germany, 976 p.

Goldhammer, R. K., 1998, Second-order accommodation cycles and points of stratigraphic turnaround; implications for high-resolution sequence stratigraphy and facies architecture of the Haynesville and Cotton Valley Lime pinnacle reefs of the East Texas Salt Basin: Houston Geological Society Bulletin, v. 40, p. 16–19.

Hancharik, J. M., 1984, Facies analysis and petroleum potential of the Jurassic Smackover Formation, western and northern areas, East Texas Basin, *in* M. W. Presley and C. H. Reed, eds., The Jurassic of East Texas: East Texas Geological Society, Tyler, p. 67–78.

Harwood, G., and C. M. Fontana, 1983, Smackover deposition and diagenesis and structural history of the Bryan's Mill area, Cass and Bowie counties, Texas (abs.): American Association of Petroleum Geologists Bulletin, v. 67, p. 1465.

Heydari, E., and C. H. Moore, 1994, Paleoceanographic and paleoclimatic controls on ooid mineralogy of the Smackover Formation, Mississippi Salt Basin: Implications for Late Jurassic seawater composition: Journal of Sedimentary Research, v. 64, p. 101–114.

Heydari, E., W. J. Wade, and L. C. Anderson, 1997, Depositional environments, organic carbon accumulation, and solar-forcing cyclicity in Smackover Formation lime mudstones, northern Gulf Coast: American Association of Petroleum Geologists Bulletin, v. 81, p. 760–774, <https://doi.org/10.1306/522B4839-1727-11D7-8645000102C1865D>.

Heydari, E., and L. Baria, 2005, A conceptual model for the sequence stratigraphy of the Smackover Formation in north-central U.S. Gulf Coast: Gulf Coast Association of Geological Societies Transactions, v. 55, p. 321–340.

IHS Markit Inc., 2022, Enerdeq browser; US exploration, production, and midstream information and analysis, <https://my.ihs.com/Energy/Products>.

Jackson, M. P. A., 1982, Fault tectonics of the East Texas Basin: Bureau of Economic Geology Geological Circular 82–4, Austin, Texas, 31 p.

Jackson, M., and S. Seni, 1983, Geometry and evolution of salt structures in a marginal rift basin of the Gulf of Mexico, East Texas: Geology, v. 11, p. 131–135.

Koepnick, R. B., D. E. Eby, and K. C. King, 1985, Controls on porosity and dolomite distribution in upper Smackover Formation (Upper Jurassic), southwestern Alabama and western Florida (abs.): American Association of Petroleum Geologists Bulletin, v. 69, p. 274.

Loucks, R. G., and M. Longman, 1982, Lower Cretaceous Ferry Lake Anhydrite, Fairway Field, East Texas: Product of shallow-subtidal deposition, *in* C. R. Handford, R. G. Loucks, and G. R. Davies, eds., Depositional and diagenetic spectra of evaporites: A core workshop: Society of Economic Paleontologists and Mineralogists Core Workshop 3, Calgary, Canada, p. 130–173.

Mancini, E. A., W. C. Parcell, and T. M. Puckett, 2003, Upper Jurassic (Oxfordian) Smackover carbonate petroleum system characterization and modeling, Mississippi Interior Salt Basin area, northeastern Gulf of Mexico, USA: Carbonates and Evaporites, v. 18, p. 125–130.

Mancini, E. A., J. C. Llinas, W. C. Parcell, M. Aurell, B. Badenas, R. R. Leinfelder, and D. J. Benson, 2004, Upper Jurassic thrombolite reservoir play, northeastern Gulf of Mexico: American Association of Petroleum Geologists Bulletin, v. 88, p. 1573–1602, <https://doi.org/10.1306/ 062104040 4017>.

Mann, S. D., 1988, Subaqueous evaporites of the Buckner Member, Haynesville Formation, northeastern Mobile County, Alabama: Gulf Coast Association of Geological Societies Transactions, v. 38, p. 187–196.

Mann, S. D., and D. C. Kopaska-Merkel, 1992, Depositional history of the Smackover-Buckner transition, eastern Mississippi Interior Salt Basin: Gulf Coast Association of Geological Societies Transactions, v. 42, p. 245–265.

Martin, R. G., 1978, Northern and eastern Gulf of Mexico continental margin: Stratigraphic and structural framework, *in* A. H. Bouma, G. T. Moore, and J. M. Coleman, eds., Framework, facies, and oil-trapping characteristics of the upper continental margin: American Association of Petroleum Geologists Studies in Geology 7, Tulsa, Oklahoma, p. 21–42.

Matyszkiewicz, J., 1993, Genesis of stromatactis in an Upper Jurassic carbonate buildup (Mlynka, Cracow region, southern Poland): Internal reworking and erosion of organic growth cavities: Facies, v. 28, p. 87–96.

Mitchell-Tapping, H. J., 1984, Depositional environment of the updip Smackover area of East Texas, *in* M. W. Presley and C. H. Reed, eds., The Jurassic of East Texas: East Texas Geological Society, Tyler, p. 79–86.

Moore, C. H., 1984, The upper Smackover of the Gulf Rim: Depositional systems, diagenesis, porosity evolution and hydrocarbon production, *in* W. P. S. Ventress, D. G. Bebout, B. F. Perkins, and C. H. Moore, The Jurassic of the Gulf rim: Proceedings of the 3rd Annual Gulf Coast Section of the Society of Economic Paleontologists and Mineralogists Foundation Research Confer-

ence, Houston, Texas, p. 282–307, <https://doi.org/10.5724/gcs.84.03.0283>.

Moore, C. H., A. Chowdhury, and L. Chan, 1988, Upper Jurassic Smackover platform dolomitization, northwestern Gulf of Mexico: A tale of two waters, *in* V. Skula and P. A. Baker, eds., Sedimentology and geochemistry of dolostones: Society of Economic Paleontologists and Mineralogists Special Publication 43, Tulsa, Oklahoma, p. 175–189.

Moore, C. H., 1997, Sequence stratigraphic framework of Upper Jurassic Oxfordian Smackover equivalents illustrated by the Humble McKean #12 core, Buckner Field, southern Arkansas, central Gulf of Mexico, USA, *in* J. Wood, ed., Sedimentary events, hydrocarbon systems: Canadian Society of Petroleum Geologists / Society of Economic Paleontologists and Mineralogists convention, Calgary, Alberta, Canada, 1–6 June 1997, p. 305-315.

Oehler, J. H., 1984, Carbonate source rocks in the Jurassic Smackover trend of Mississippi, Alabama, and Florida, *in* J. G. Palacas, ed., Petroleum geochemistry and source rock potential of carbonate rocks: American Association of Petroleum Geologists Studies in Geology 18, Tulsa, Oklahoma, p. 63–69, <https://doi.org/10.1306/St18443>.

Oschmann, W., 1993, Environmental oxygen fluctuations and the adaptive response of marine benthic organisms: Journal of the Geological Society of London, v. 150, p. 187–191.

Pearson, O. N., 2011, Undiscovered hydrocarbon resources in the US Gulf Coast Jurassic Norphlet and Smackover formations: Gulf Coast Association of Geological Societies Transactions, v. 61, p. 329–340.

Pilger, R. H., Jr., 1981, The opening of the Gulf of Mexico: Implications for the tectonic evolution of the northern Gulf Coast: Gulf Coast Association of Geological Societies Transactions, v. 31, p. 377–381.

Pindell, J., and L. Kennan, 2001, Kinematic evolution of the Gulf of Mexico and Caribbean, *in* R. H. Fillon, N. C. Rosen, P. Weimer, A. Lowrie, H. Pettingill, R. L. Phair, H. H. Roberts, and H. H. van Hoom, eds., Petroleum systems of deep-water basins—Global and Gulf of Mexico experience: Proceedings of the 21st Annual Gulf Coast Section of the Society of Economic Paleontologists and Mineralogists Foundation Research Conference, Houston, Texas, p. 193–220, <https://doi.org/10.5724/gcs.01.21.0193>.

Pratt, B. R., 2001, Calcification of cyanobacterial filaments: *Girvanella* and the origin of lower Paleozoic lime mud: Geology, v. 29, p. 763–766, <https://doi.org/10.1130/0091-7613(2001)029<0763:COCFGA>2.0.CO;2>.

Reading, H. G., and J. D. Collinson, 1996, Clastic coasts, *in* H. G. Reading, ed., Sedimentary environments: Processes, facies and stratigraphy: Blackwell Science, Oxford, U.K., p. 154– 258.

Rowe, H. D., N. Hughes, and K. Robinson, 2012, The quantification and application of handheld energy-dispersive x–ray fluorescence (ED–XRF) in mudrock chemostratigraphy and geochemistry: Chemical Geology, v. 324–325, p. 122–131, <https://doi.org/10.1016/j.chemgeo.2011.12.023>.

Salvador, A., 1987, Late Triassic-Jurassic paleogeography and origin of Gulf of Mexico Basin: American Association of Petroleum Geologists Bulletin, v. 71, p. 419–451.

Sassen, R., 1990, Geochemistry of carbonate source rocks and crude oils in Jurassic salt basins of the Gulf Coast, *in* Gulf Coast oils and gases: Their characteristics, origin, distribution, and exploration and production significance: Program with Extended and Illustrated Abstracts of the 9th Annual Gulf Coast Section of the Society of Economic Paleontologists and Mineralogists Foundation Research Conference, p. 11–22, <https://doi.org/10.5724/gcs.90.09.0011>.

Schieber, J., P. K. Bose, P. G. Eriksson, S. Banerjee, S. Sarkar, W. Altermann, and O. Catuneanu, 2007, Atlas of microbial mat features preserved within the siliciclastic rock record, v. 2: Elsevier, Amsterdam, The Netherlands, 311 p.

Schreiber, B. C., R. Catalano, and E. Schreiber, 1977, An evaporitic lithofacies continuum: Latest Miocene (Messinian) deposits of Salemi Basin (Sicily) and a modern analog, *in* J. H. Fisher, ed., Reefs and evaporites—Concepts and depositional models: American Association of Petroleum Geologists Studies in Geology 5, Tulsa, Oklahoma, p. 169–180, <https://doi.org/10.1306/St5390C9>.

Scotese, C. R., 2014, Atlas of Jurassic paleogeographic maps: Mollweide Project, PALEOMAP Project, Evanston, Illinois, PALEOMAP Atlas for ArcGIS, v. 4, The Jurassic and Triassic, Map 32–42.

Stewart, S. K., 1984, Smackover and Haynesville facies relationships in north-central East Texas, *in* M. W. Presley and C. H. Reed, eds., The Jurassic of East Texas: East Texas Geological Society, Tyler, p. 56–62.

Thompson, J. B., and F. G. Ferris, 1990, Cyanobacterial precipitation of gypsum, calcite, and magnesite from natural alkaline lake water: Geology, v. 18, p. 995–998.

Van Wagoner, J. C., R. M. Mitcham, K. M. Campion, and V. D. Rahmanian, 1990, Siliciclastic sequence stratigraphy in well logs, cores and outcrops: Concepts for high-resolution correlation of time and facies: American Association of Petroleum Geologists Methods in Exploration Series 7, Tulsa, Oklahoma, 55 p.

Wade, W. J., and C. H. Moore, 1993, Jurassic sequence stratigraphy of southwest Alabama: Gulf Coast Association of Geological Societies Transactions, v. 43, p. 431–443.

Walker, J. D., J. W. Geissman, S. A. Bowring, and L. E. Babcock, compilers, 2018, GSA geologic time scale, version 5.0: Geological Society of America, Boulder, Colorado, <https://doi.org/10.1130/2018.CTS005R3C>.

Wanless, H. R., L. P. Tedesco, and K. M. Tyrrell, 1988, Production of subtidal tubular and surficial tempestites by Hurricane Kate, Caicos Platform, British West Indies: Journal of Sedimentary Petrology, v. 58, p. 739–750.

Warren, J. K., 2006, Evaporites: Sediments, resources, and hydrocarbons: Springer, New York, 1035 p.

Wilkinson, S., 1984, Upper Jurassic facies relationships and their interdependence on salt tectonism in Rains, Van Zandt, and adjacent counties, East Texas, *in* M. W. Presley and C. H. Reed, eds., The Jurassic of East Texas: East Texas Geological Society, Tyler, p. 153–156.

Wood, M. L., and J. L. Walper, 1974, The evolution of the Interior Mesozoic Basin and the Gulf of Mexico: Gulf Coast Association of Geological Societies Transactions, v. 24, p. 31–41.

Yang, B., R. G. Gerdes, and J. Choi, 2015, The newly emerging lower Smackover (Brown Dense) Formation: Its geologic characteristics and exploration potential: Unconventional Resources Technology Conference, San Antonio, Texas, <https://doi.org/10.15530/URTEC-2015-2150052>.